

# **Innovative Use of High-Resolution K (HRK) Logging for Optimizing Dewatering System Designs**

Year #1 Report for Field Work at Scoggins Dam, Oregon

Prepared for



— BUREAU OF —  
RECLAMATION

Gaisheng Liu, Steve Knobbe, and James Butler  
Kansas Geological Survey, University of Kansas  
1930 Constant Ave., Lawrence, KS 66047

[gliu@ku.edu](mailto:gliu@ku.edu)  
Phone: 785-864-2115

**August 31, 2024**

# TABLE OF CONTENTS

LIST OF FIGURES .....	III
ACKNOWLEDGMENTS .....	IV
1. INTRODUCTION.....	1
2. HRK APPLICATION AT THE SCOGGINS DAM RESEARCH SITE.....	2
3. HRK RESULTS AT THE SCOGGINS DAM RESEARCH SITE .....	3
4. NEXT STEPS .....	4
APPENDIX .....	14
REFERENCES.....	38

## LIST OF FIGURES

**Figure 1.** Schematic of the DP Permeameter (DPP). The injection lines at the pressure transducer ports were added during the development of the high-resolution K (HRK) tool.

**Figure 2.** Prototype high-resolution K tool: (A) Picture showing the bottom injection screen with the two pressure transducers inset into the rod above the screen, and (B) expanded view of the pressure transducer screen. Water is injected through the bottom screen and both transducer ports during probe advancement.

**Figure 3.** Map of Scoggins Dam Research Site and the locations of four HRK profiles. See Figure 4 for detailed HPT profiles along A–A’.

**Figure 4.** Locations of four HRK profiles relative to previous HPT profiles. HRK1 and HRK2 are in a relatively high-K zone with many interbedded thin layers of sands and silts/clays (labeled as zone 1). HRK4 is in a very low-K zone (zone 3). HRK3 is in a transition zone (zone 2) with relatively higher K at shallow depths. The solid red line indicates the top of sandstone bedrock where probe advancement was not possible. The dashed red line indicates the potential boundary between more recent coarse deposits in high-energy settings and earlier Quaternary fine-grained deposits in low-energy settings.

**Figure 5.** HRK principles of operation. During profiling, a utility pump supplies water from a source tank (S). Because water must be injected at a relatively high rate for DPP injection tests, a piston pump (A) is used to increase water supply pressure. The flow rates for the bottom injection (Q), upper pressure port (F), and lower pressure port (G) are set in the flow control box (B). The flow rates are monitored by flowmeters in (B) at the surface, while the injection pressures for the upper and lower ports are measured by a transducer package (E) in the probe downhole. The injection pressure for the bottom screen is measured in the flow control box. The trunkline (D) connects the downhole probe to the data acquisition box (C), which can convert the electrical signals into digital formats for real-time display on a field laptop.

**Figure 6.** DPP example test at a depth of 40 ft in the HRK1 profile at Scoggins.

**Figure 7.** Data analyses of the DPP test at a depth of 40 ft in the HRK1 profile: (A) Injection rate (green) and injection-induced pressure head difference between the upper and lower transducer ports (blue), and (B) individual pressure heads measured at the upper (orange) and lower (blue) ports.

**Figure 8.** Estimated K values from four HRK profiles at Scoggins: (A) HRK1, (B) HRK2, (C) HRK3, and (D) HRK4.

## **ACKNOWLEDGMENTS**

The research described in this year 1 project report was funded by the U.S. Bureau of Reclamation through the Science and Technology Program. Mr. Jong Kang and other USBR staff are gratefully acknowledged for their assistance and support.

# 1. Introduction

Effective design of dewatering systems continues to be hampered by the difficulty in characterizing hydraulic properties of subsurface formations at the resolution, accuracy, and speed that are needed to significantly improve the understanding of groundwater flow behavior at many USBR dam sites. Traditional site characterization approaches, such as pumping tests, slug tests, or flowmeter profiling, have proven to be of limited utility when the aquifer materials are highly heterogeneous with preferential flow channels occurring at the scale of decimeters or smaller. To address this concern, a series of higher-resolution approaches have been developed based on direct-push (DP) technology (McCall et al., 2005; Butler et al., 2007; Dietrich et al., 2008; Liu et al., 2009; Maliva, 2016; Liu et al., 2019; McCall and Christy, 2020; Morozov et al., 2024).

Geoprobe® developed the DP-based Hydraulic Profiling Tool (HPT) system to evaluate the lithologic character and hydraulic behavior of unconsolidated materials (McCall and Christy 2010). HPT combines continuous DP injection logging (DPIL; Dietrich et al., 2008) with electric conductivity (EC) profiling (Geoprobe Systems, 2007). As the tool is advanced, water is injected into the subsurface continuously through a screen. The injection rate is monitored at the surface, while the pressure is measured directly behind the screen in the probe downhole. The ratio of injection rate to injection pressure is used for K estimation, while the EC measurements provide a good indicator of lithology (sands and gravels have low EC, while silts and clays generally have high EC). HPT profiling is very rapid in the field, and up to six profiles of 12 m in length can be obtained in a day under good conditions. HPT produces a K estimate every 0.015 m, thus providing unprecedentedly high-resolution information about aquifer K in the saturated zone across the entire interval traversed during probe advancement. Due to the instrument (e.g., flowmeter and pressure sensor ranges and resolutions) and procedural (injection during probe advancement) constraints, HPT has limits at both the upper and lower ends of its K measurement, and the measurable range is estimated to be 0.03 to 25 m/d for the current system (Geoprobe Systems, 2010). Profiling hydraulic conductivity (K) variations with the HPT has now been established as a standard practice by the American Society for Testing and Materials (ASTM, 2016).

The DP Permeameter (DPP) is a tool that can be used to obtain reliable K estimates at a resolution that is coarser than HPT but finer than most other borehole approaches (Butler et al., 2007; Liu et al., 2008). It consists of a short cylindrical screen attached to the lower end of a DP rod and two pressure transducers inset into the rod above the screen (Figure 1). During advancement, water is continuously injected through the injection screen to prevent clogging. After the measurement depth is reached, advancement ceases, and water injection is stopped to allow the heads in the aquifer to recover to background conditions. After the aquifer heads recover, a series of short-term step injections are performed, and K is estimated from the spherical form of Darcy's Law using the injection rate and the injection induced pressure responses at the two transducers (Butler et al., 2007),

$$K_{DPP} = \frac{Q}{4\pi(\Delta h_1 - \Delta h_2)} \left( \frac{1}{z_1} - \frac{1}{z_2} \right), \quad (1)$$

where Q is injection rate,  $\Delta h_1$  and  $\Delta h_2$  are the injection-induced pressure head changes at pressure transducers PT1 and PT2, and  $z_1$  and  $z_2$  are the distances from PT1 and PT2 to the injection screen, respectively (Figure 1).  $K_{DPP}$  is a weighted average over the interval between

the screen and the farthest transducer, which is approximately 0.4 m for the current prototype DPP tool; material outside of that interval has little influence on the estimated K (Liu et al., 2008). The major advantage of the DPP is that it only requires steady-shape conditions (constant hydraulic gradient with time) as opposed to techniques that require the attainment of steady-state condition (constant head with time). The steady-shape analysis also allows for shorter test times in the field. In addition, the resulting K estimates are not sensitive to the low-K skin that can potentially develop due to material compaction during tool advancement. Background water-level fluctuations due to regional stresses (e.g., well pumping, stream stage changes) also have a minimal impact on DPP results because the fluctuations are largely canceled out using the steady-shape analysis.

The HRK (high-resolution K) tool was developed to better realize the potential of DPIL (the injection logging component of HPT) and DPP by coupling them into a single probe (Liu et al., 2009). The tool has a similar appearance to the DPP (i.e., two pressure transducer ports above the bottom injection screen; Figure 2). The difference is that water is injected through both pressure transducer ports during tool advancement (water also is injected through the bottom screen to prevent clogging); the DPP only injected water through the bottom screen during advancement. By injecting water through the transducer ports and measuring injection responses during tool advancement, the HRK tool essentially functions in the continuous DPIL mode. At selected depth intervals, tool advancement ceases and the DPP injection tests are performed. The DPIL measurements can be converted into K estimates using the regression relation developed for HPT by Geoprobe (Geoprobe Systems, 2007). Alternatively, as the DPIL and DPP measurements are collocated, the DPP data can be used to directly transform the DPIL ratios into K through numerical simulations (Liu et al., 2009).

In this project, HPT, nuclear magnetic resonance (NMR), and HRK loggings were applied at the Scoggins Dam research site in Oregon during May 11–15, 2024. A Geoprobe report presented the HPT and NMR results. This report will focus on the HRK field results.

## **2. HRK Application at the Scoggins Dam Research Site**

Four HRK profiles were conducted at the Scoggins Dam research site (Figure 3). The unconsolidated sediments overlying the sandstone bedrock at the site can be divided into two geologic units: highly permeable stream channel deposits with a significant portion of sands and gravels interbedded with thin lenses of clays and silts (e.g., zone 1 and the upper interval of zone 2 in Figure 4) and low-permeability fine-grained silts and clays with minimal sands and gravels (lower interval of zone 2 and zone 3 in Figure 4). The bottoms of various DP profiles stop at the top of the bedrock where probe advancement was not possible due to the sandstone. Based on the layer sequence observed from the HPT profiles, it is likely the fine-grained unit was deposited in low-energy riparian settings with higher stream stage and slower current during the earlier Quaternary period. The permeable coarse unit was primarily associated with more recent high-energy stream events (e.g., fast streamflow during flooding) such that it overlies the fine-grained unit in the transition zone.

The field operation of HRK is similar to that of the HPT (Figure 5). Prior to profiling, the HRK trunkline must be pre-strung through all the connection rods, and the pressure sensors for both the upper and lower ports must be tested in a calibration pipe. After the sensors pass the quality-

control tests, water injection is turned on for the bottom screen (typically at 400 mL/min) and both transducer ports (typically 150 to 200 mL/min). The zero depth is set at the middle point between the two transducer ports. The “trigger on” button in the data acquisition software needs to be clicked to record the depth profiles of upper and lower port injection pressures and rates. During advancement, the HRK tool essentially functions as the injection logging component of the HPT. Upon reaching a depth interval suitable for DPP testing (typically in more permeable zones as the testing time can be several hours or more in low-permeability zones), the injection is turned off for all three lines (screen and two ports) so that the injection pressures can dissipate. In field operations, the viewing window needs to be switched from “depth” to “time” mode and the time recording button clicked before all the injection valves are closed. This way, the full pressure recovery after shutting off water injection is saved and can be observed in real time. Under normal circumstances, DPP injection tests are performed only after the water levels return to background conditions. At Scoggins, however, due to time constraints in the field, most DPP tests were conducted as soon as both the upper and lower port injection pressures had largely dissipated and were showing a smooth trend that could be removed during subsequent data analyses.

Figure 6 shows an example DPP test performed at Scoggins. The test was performed at a depth of 40 ft in the HRK1 profile. Upon reaching the test depth at about 5800 seconds, all injection ceased and the pressure recovery for the upper and lower transducer ports was monitored. The DPP test started at a time of 6440 seconds after the pressures at both transducer ports displayed a similar smooth trend.

Figure 7 shows the data analyses of the example DPP test at a depth of 40 ft in the HRK1 profile. Three injection rates were used. For the first injection rate (about 230 mL/min), the injection-induced pressure head difference (i.e., the pressure head difference between the two transducers during injection minus the pressure head difference prior to injection) was 0.21 m. The injection-induced pressure head difference in the first rate determined how the injection rate was adjusted in the next step. Because 0.21 m is a relatively small value, the injection rate was raised to around 450 mL/min in the second step. In the third step, the injection rate was adjusted back to the level of the first rate to check whether the injection-induced pressure returned to the level observed during the first rate. For the three rates shown in Figure 7, the calculated K values are 0.71, 0.65, and 0.68 m/d, respectively. The consistency between the K estimates from the three rates observed here is a good indication of the reliability of DPP results; a lack of consistency could be due to sensor instability (e.g., air bubbles in the injection water can cause unstable sensor readings) or formation alteration during DPP testing (e.g., vertical channeling along the probe surface).

### **3. HRK Results at the Scoggins Dam Research Site**

Figure 8 shows the estimated K values from the four HRK profiles performed at Scoggins. Each profile includes the continuous DPIL K estimates, which are computed from the ratio of injection rate over pressure measured from the upper transducer port, and the DPP test K values at selected depths. In HRK1, four DPP tests were performed at depths of 12.5, 20.4, 35.1 and 40.0 ft; in HRK2, twelve DPP tests were performed at depths of 10.7, 12.6, 14.6, 17.7, 21.4, 29.8,

31.8, 34.2, 39.7, 41.5, 43.3, and 44.1 ft; in HRK3, three DPP tests were performed at depths of 10.3, 13.5, and 24.6 ft; in HRK4, only one DPP test was performed at a depth of 7.2 ft as much of the formation is dominated by silts and clays and the permeability is too low for conducting DPP tests in a reasonable time.

The continuous DPIL K estimates are computed using the regression relationship determined for HPT by Geoprobe (Geoprobe Systems, 2010),

$$K_{\text{DPIL}} [\text{ft/d}] = 21.14 \times \ln(Q/P) - 41.71, \quad (2)$$

where Q is the injection rate at the upper transducer port (mL/min) and P is injection pressure at the upper port after removing hydrostatic pressure from the total pressure measured by the transducer. As discussed earlier, the estimated  $K_{\text{DPIL}}$  for current HPT has a lower and upper limit of 0.03 and 25 m/d, respectively.

Overall, the continuous DPIL and DPP K estimates are consistent with each other at Scoggins (Figure 8). Like previous HPT profiles at the site, the formation materials at HRK1, HRK2, and the shallow interval of HRK3 are relatively permeable, which is shown by the estimated K values from both DPIL and DPP. It is interesting to note that the permeable formation is not homogeneous at Scoggins, but instead has many thin interbedded layers of low-permeability silts and clays. This means that despite the significant portion of permeable sands and gravels in this geological unit, vertical hydraulic connection may not be strong due to silt and clay layers acting as flow barriers. Therefore, in dewatering system designs, lateral flow through the sand and gravel layers should be the major focus.

There are two important observations from the DPP results. First, the highest K estimates were detected near the bottom of HRK2. This is consistent with the finding from previous USBR investigations conducted at the site that indicated the basal formation of sand and gravel unit is the most permeable. Although HRK1 is in the same geological unit as HRK2, it does not have such a high-K zone at the bottom of the profile, again showing significant aquifer heterogeneity at the site. Second, the DPP K estimate at a depth of 7 ft in HRK4 appears to be too large as compared to the DPIL profile. This large overestimation of K could be due to the presence of a very thin low-K layer separating the tip screen from both pressure transducer ports (see the thin low-K layer between depths 7.9 and 8.3 ft in the continuous K profile of HRK4 on Figure 8D). When such a layer exists, it will significantly obstruct the upward movement of injection pressure from the screen to both transducer ports and cause the estimated K to be larger than actual (in a high-K zone, the pressure response to injection is small). Such a case has rarely been observed in previous HRK field studies, but numerical simulations have shown that it can be a possible explanation if the DPP produces a large overestimation of K in highly layered systems (Liu et al., 2008).

#### **4. Next Steps**

One major challenge in the HRK field operation at Scoggins was that air trapping occurred more significantly than typical, particularly during the later morning and afternoon hours when the air temperature increased. The atypical air trapping was likely due to two factors. First, as the temperature increased, air solubility decreased. As a result, dissolved air coalesced and formed bubbles in the source water. Second, the utility pump in the source tank was not able to produce sufficient water supply pressure to the HRK pump on a consistent basis. This was particularly noticeable immediately after the HRK pump was turned on at the beginning of a DPP test at certain test intervals. Due to the insufficient supply pressure from the utility pump, the pressure gage in the HRK pump fluctuated significantly and the system produced significant noise and vibration, which usually lasted for several seconds before it returned to normal. We suspected that air bubbles were injected into the formation during that pressure fluctuation period and the injected bubbles caused the pressure measurements at both transducer ports to be unsteady during DPP tests. Based on our previous HRK studies, the transducer package used in the downhole probe was very sensitive to air bubbles that could be trapped inside it.

To overcome the air trapping issue in future HRK work, we are planning to install a de-airing system for the source water tank. We have previously used a de-airing system for a low-permeability HPT system developed by the KGS. However, the amount of water that was needed for HPT operation was much less than that for HRK. Therefore, unlike the HPT de-airing system that is only turned on at about the same time as the pre-logging quality control tests, the de-airing system for HRK would need to be turned on for several hours ahead of profiling. In addition, a more powerful utility pump will be used for future HRK field applications to ensure the water supply pressure to the HRK pump is consistently sufficient during DPP tests.

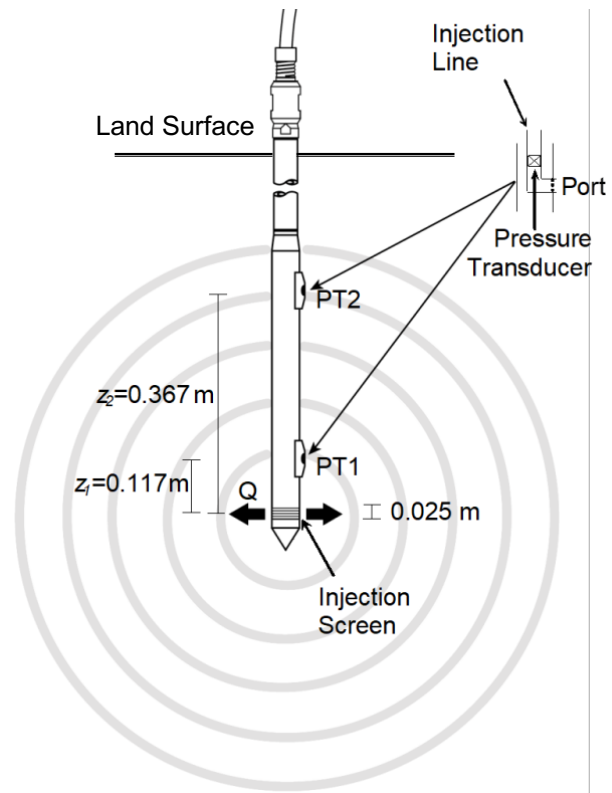


**Figure 1.** Schematic of the DP Permeameter (DPP). The injection lines at the pressure transducer ports were added during the development of the high-resolution K (HRK) tool.



(A)



(B)

**Figure 2.** Prototype high-resolution K tool: (A) Picture showing the bottom injection screen with the two pressure transducers inset into the rod above the screen, and (B) expanded view of the pressure transducer screen. Water is injected through the bottom screen and both transducer ports during probe advancement.

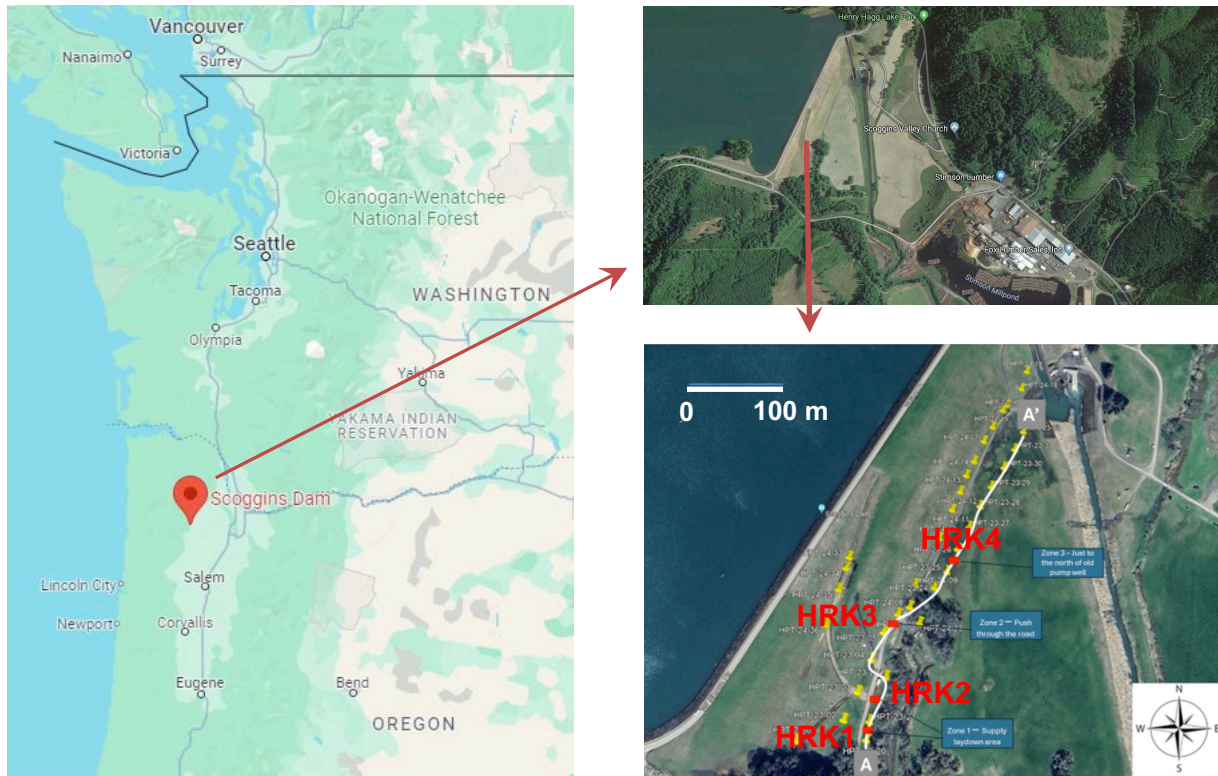


**Figure 3.** Map of Scoggins Dam Research Site and the locations of four HRK profiles. See Figure 4 for detailed HPT profiles along A–A’.

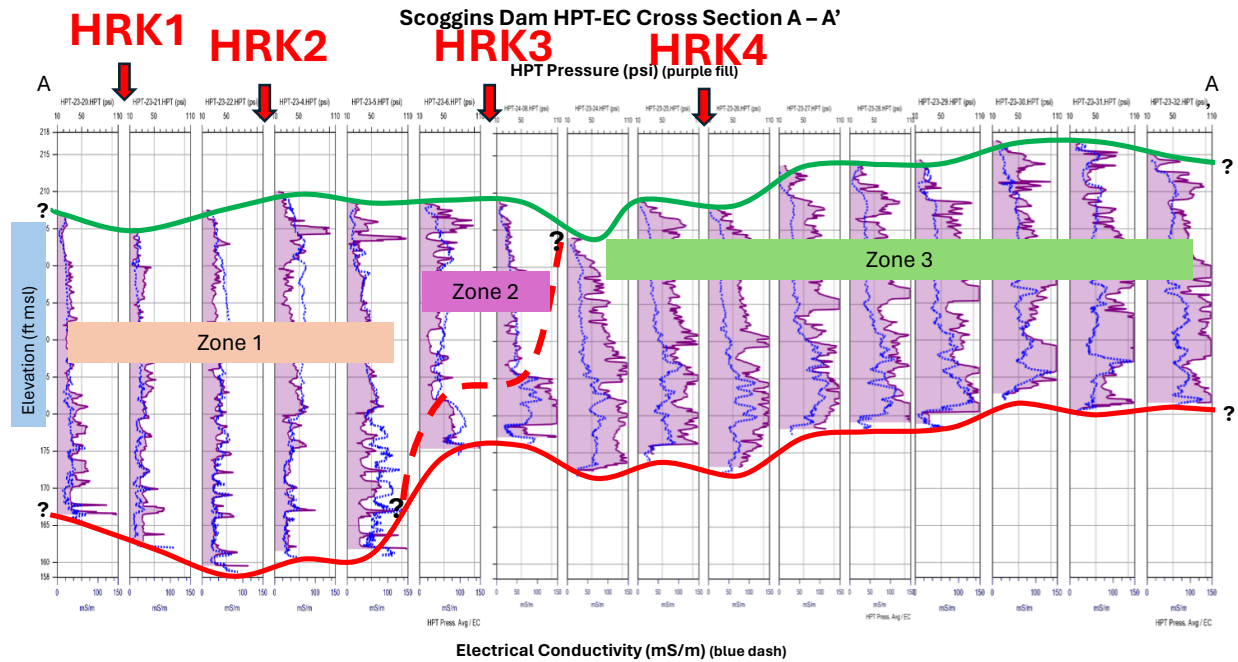


**Figure 4.** Locations of four HRK profiles relative to previous HPT profiles. HRK1 and HRK2 are in a relatively high-K zone with many interbedded thin layers of sands and silts/clays (labeled as zone 1). HRK4 is in a very low-K zone (zone 3). HRK3 is in a transition zone (zone 2) with relatively higher K at shallower depths. The solid red line indicates the top of sandstone bedrock where probe advancement ceased. The dashed red line indicates the potential boundary between more recent coarse deposits in high-energy settings and earlier Quaternary fine-grained deposits in low-energy settings.

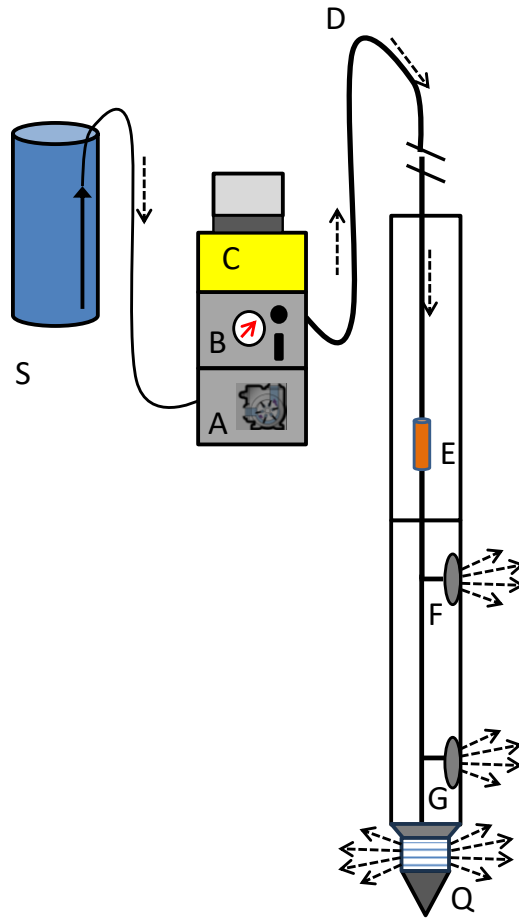


**Figure 5.** HRK principles of operation. During profiling, a utility pump supplies water from a source tank (S). Because water must be injected at a relatively high rate, a piston pump (A) is used to increase water supply pressure. The flow rates for the bottom injection (Q), upper pressure port (F), and lower pressure port (G) are set in the flow control box (B). The flow rates are monitored by flowmeters in (B) at the surface, while the injection pressures for the upper and lower ports are measured by a transducer package (E) in the probe downhole. The injection pressure for the bottom screen is measured in the flow control box. The trunkline (D) connects the downhole probe to the data acquisition box (C), which can convert the electrical signals into digital formats for real-time display on a field laptop.

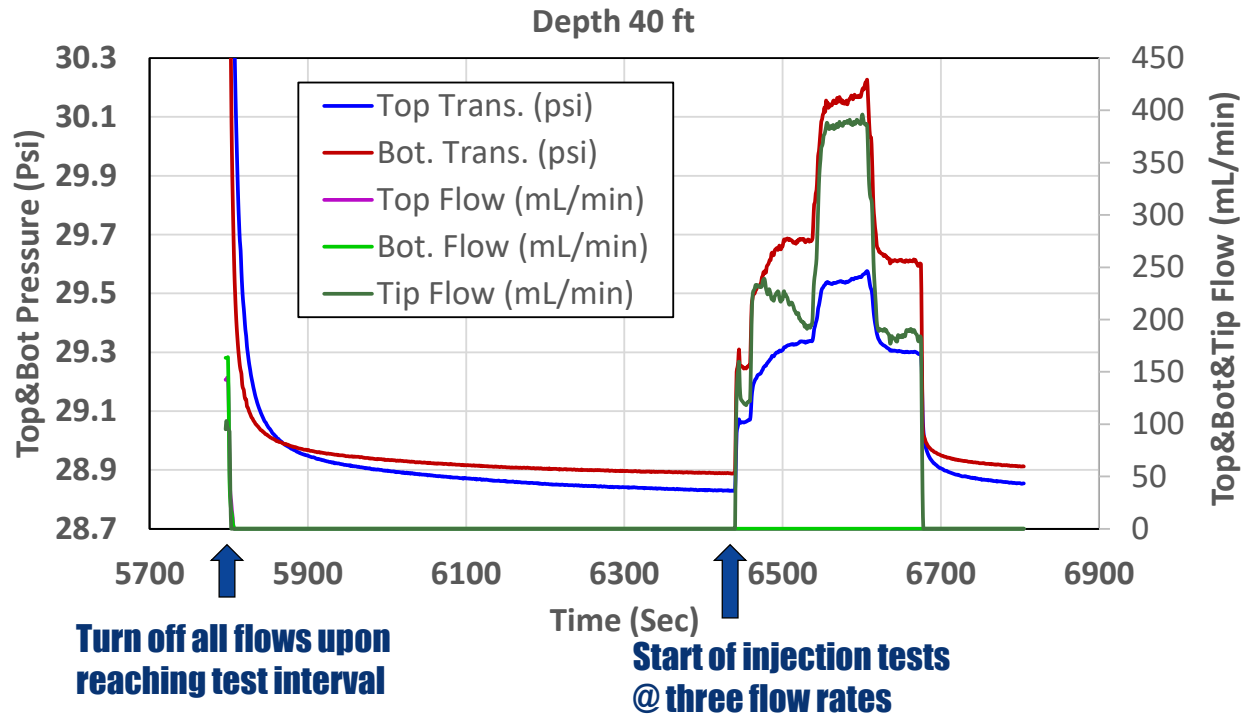


**Figure 6.** DPP example test at a depth of 40 ft in the HRK1 profile at Scoggins.

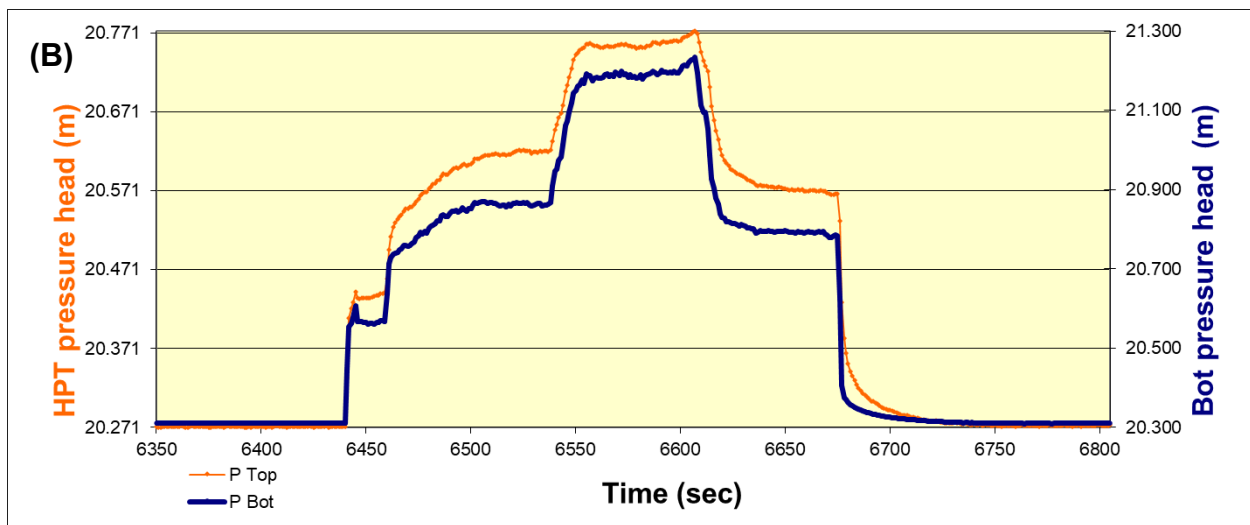
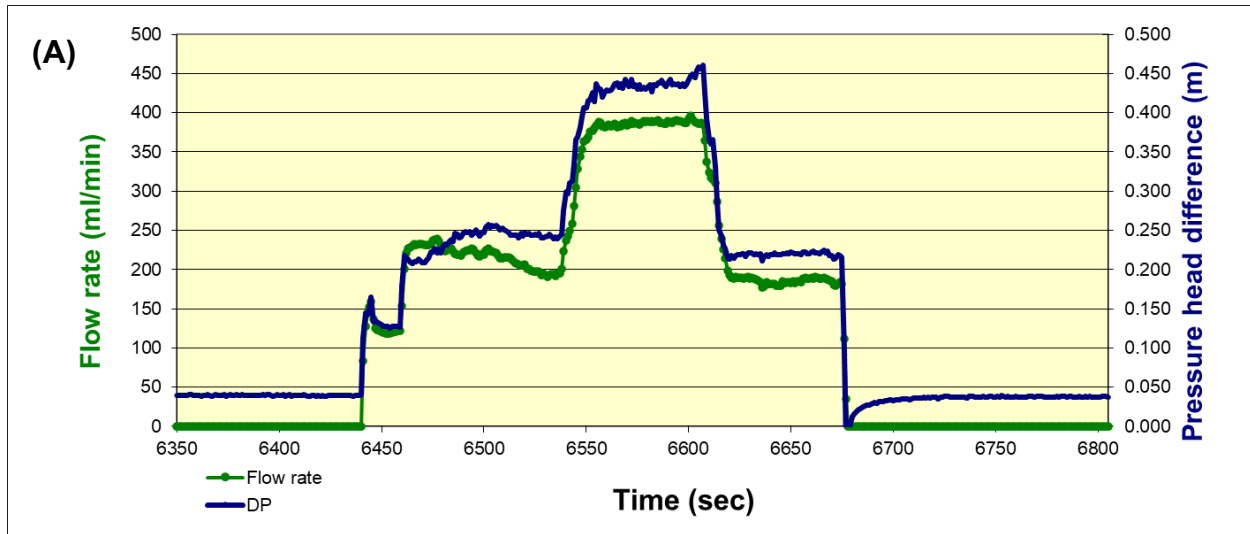


**Figure 7.** Data analyses of the DPP test at a depth of 40 ft in the HRK1 profile: (A) Injection rate (green) and injection-induced pressure head difference between the upper and lower transducer ports (blue), and (B) individual pressure heads measured at the upper (orange) and lower (blue) ports.

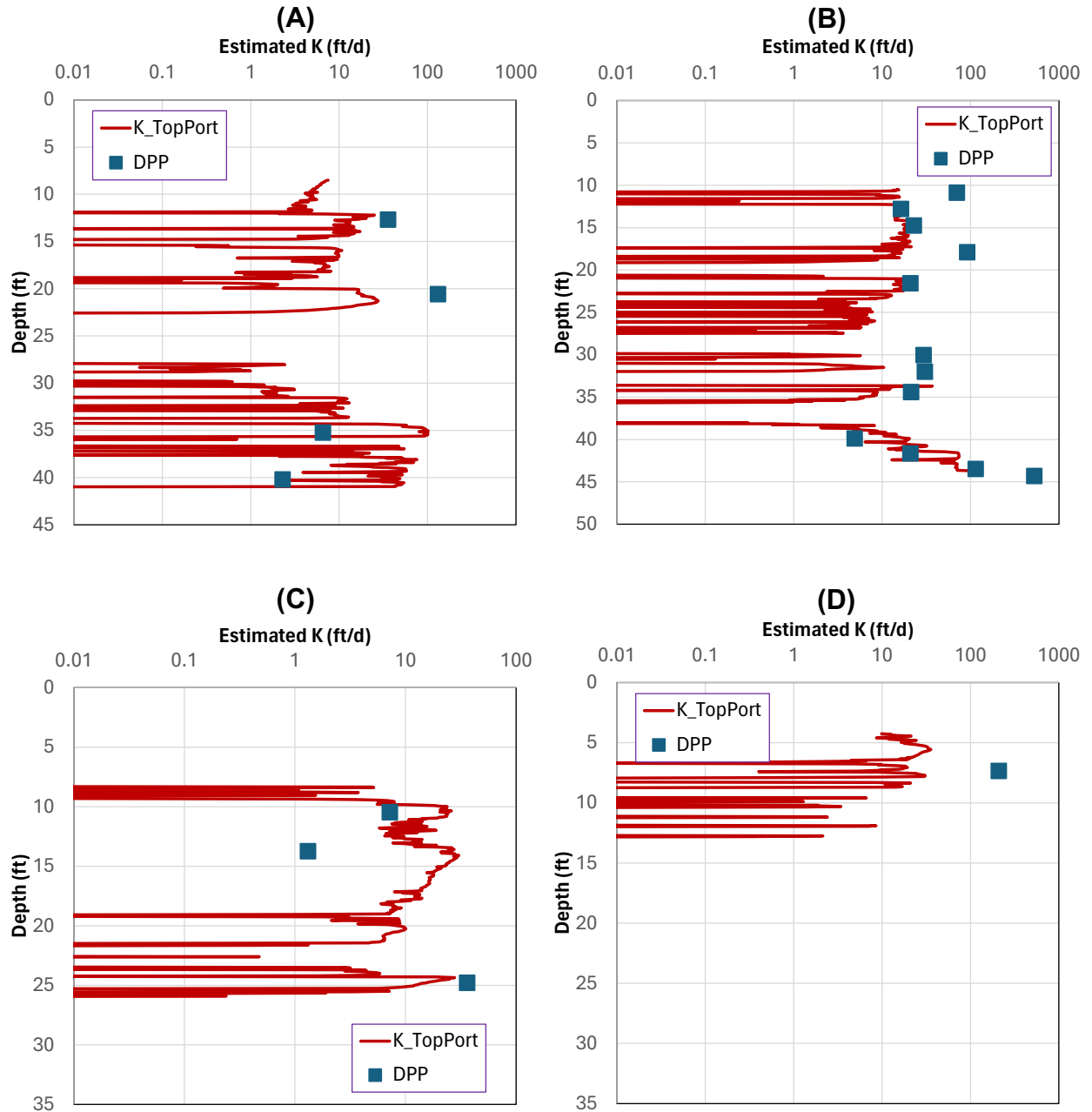


**Figure 8.** Estimated K values from four HRK profiles at Scoggins: (A) HRK1, (B) HRK2, (C) HRK3, and (D) HRK4.

## APPENDIX

As described in the main report, most of the DPP tests at Scoggins were performed before the tool advancement-generated pressure disturbances were completely dissipated. Therefore, background pressure trends were manually analyzed and removed before the DPP test data were used for K estimation. The individual test data analyses are compiled below for selected test intervals for profiles HRK1 to HRK4.

### A.1. HRK1 Profile

Figure A1 shows the measured pressure and injection rate at the upper transducer port during HRK1 continuous profiling. Figure A2 shows the hydrostatic pressure line for the HRK1 depth profile. The equation of the fitted line is used for computing the hydrostatic pressure below the water table. Figure A3 shows the upper transducer port corrected pressure and estimated DPIL K for the HRK1 profile.

Figure A4 shows the measured pressure at the upper transducer and lower transducer ports, flow rate at the upper transducer and lower transducer ports, and flow rate at the tip screen before and during the DPP test at a depth of 20.4 ft in HRK1. Figure A5 shows the measured pressure at the lower transducer port and estimated background pressure trend for the DPP test at a depth of 20.4 ft in HRK1. The green line is the flow injection rate during the DPP test for reference. The difference between the measured and background pressure lines is considered to be the injection-induced pressure response used in K estimation. Figure A6 shows the measured pressure at the upper transducer port and estimated background pressure trend for the DPP test at a depth of 20.4 ft in HRK1. Figure A7 shows the tip flow rate and pressure difference between the upper and lower transducer ports and background trend-removed pressures at the individual transducer ports for the DPP test at a depth of 20.4 ft in HRK1. Note that in Figure A7, the label “P Top” is the same as “HPT pressure head” on the left axis, which means the pressure measured at the upper transducer port PT2 (see Figure 1). The DPP K estimate is obtained using the average flow rate and injection-induced pressure difference (see equation 1).

Figures A8 to A11 show similar information for the DPP test performed at a depth of 40 ft in the HRK1 profile.

### A.2. HRK2 Profile

Figures A12–A14 show the results of the DPIL depth profile of HRK2. Figures A15–A22 show the DPP test results at depths of 41.45 and 44.1 ft in HRK2.

### A.3. HRK3 Profile

Figures A23–A25 show the results of the DPIL depth profile of HRK3. Figures A26–A29 show the DPP test results at a depth of 13.55 ft in HRK3.

### A.4. HRK4 Profile

Figures A30–A32 show the results of the DPIL depth profile of HRK4. Figures A33–A36 show the DPP test results at a depth of 7.15 ft in HRK4.

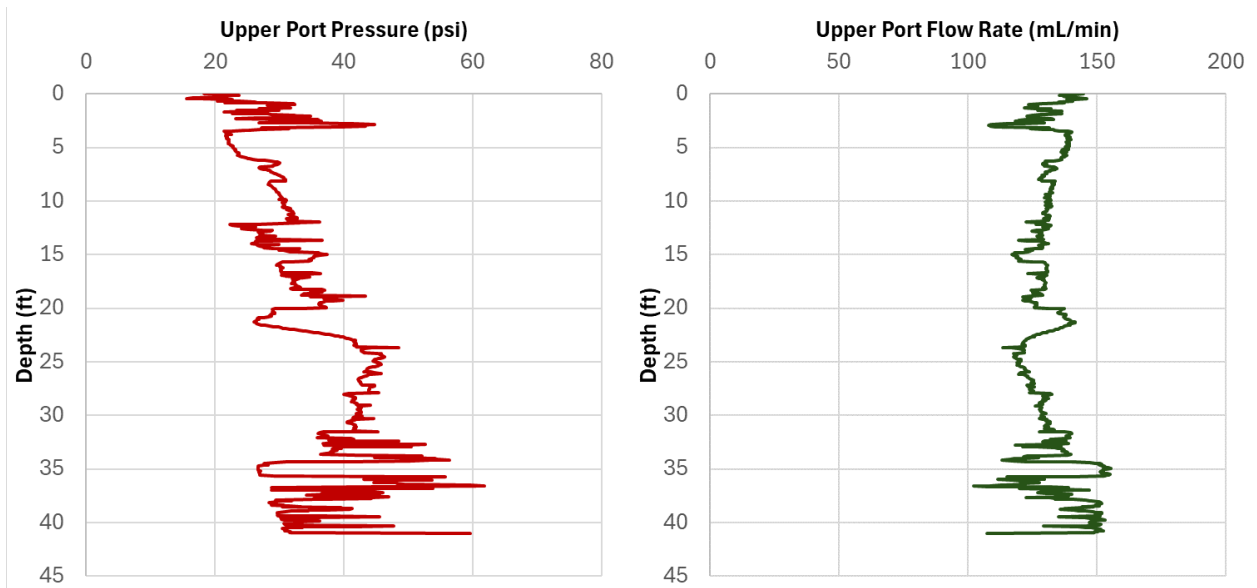


**Figure A1.** Measured pressure (left) and injection rate (right) at the upper transducer port during HRK1 continuous profiling.

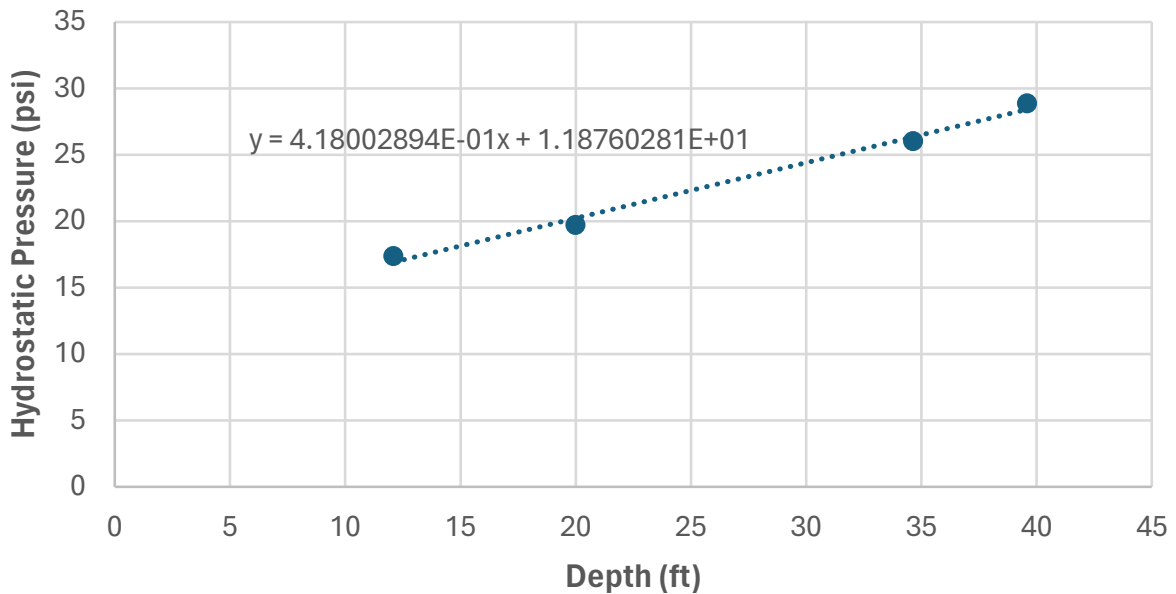


**Figure A2.** Hydrostatic pressure line for the HRK1 depth profile. The depth to the water table is estimated to be 8.5 ft. The equation of the fitted line is used for computing the hydrostatic pressure below the water table (the hydrostatic pressure at the water table is equal to atmospheric pressure).

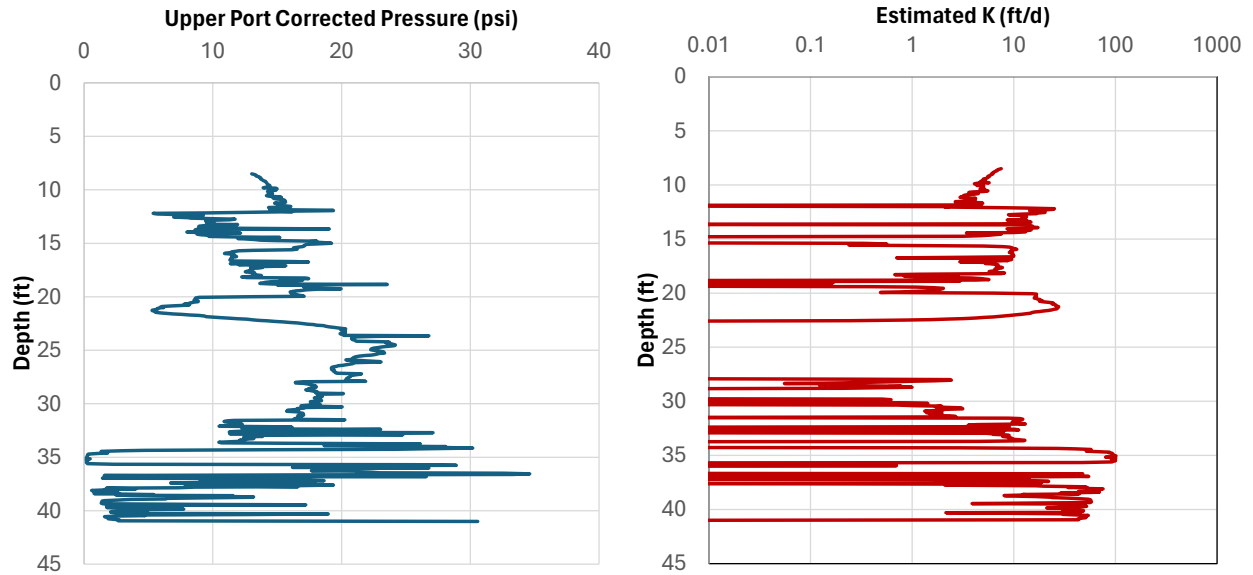


**Figure A3.** Upper transducer port corrected pressure (left) and estimated DPIL K (right) for the HRK1 profile.

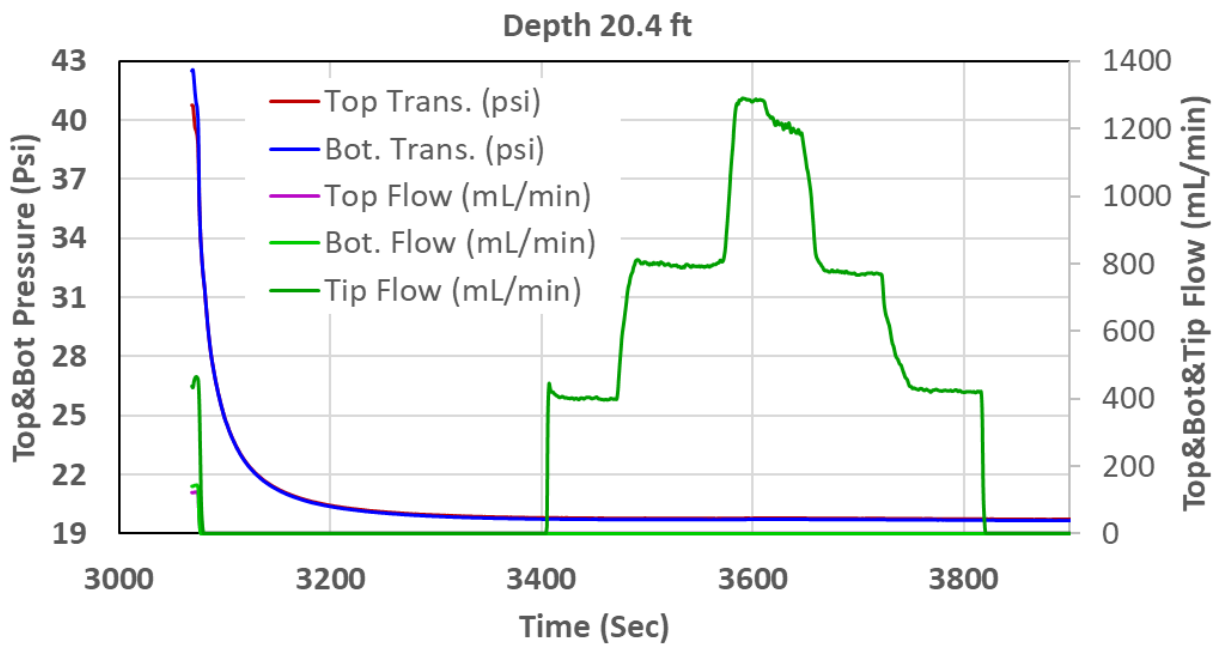


**Figure A4.** Measured pressure at the upper transducer port (Top Trans.) and lower transducer port (Bot. Trans.), flow rate at the upper transducer port (Top Flow) and lower transducer port (Bot. Flow), and flow rate at the tip screen (Tip Flow) before and during the DPP test at a depth of 20.4 ft in HRK1.

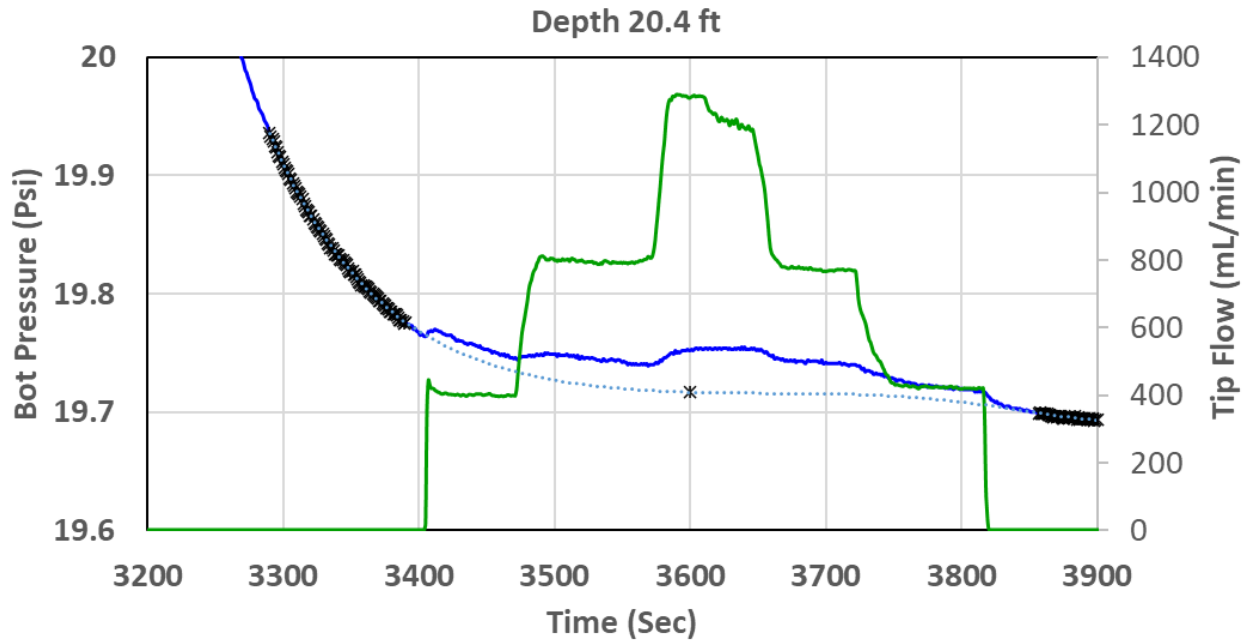


**Figure A5.** Measured pressure at the lower transducer port (solid blue line) and estimated background pressure trend (dotted line) for the DPP test at a depth of 20.4 ft in HRK1. The green line is the flow injection rate during the DPP test. The difference between the measured and background pressure lines is considered to be the injection-induced response used in K estimation.

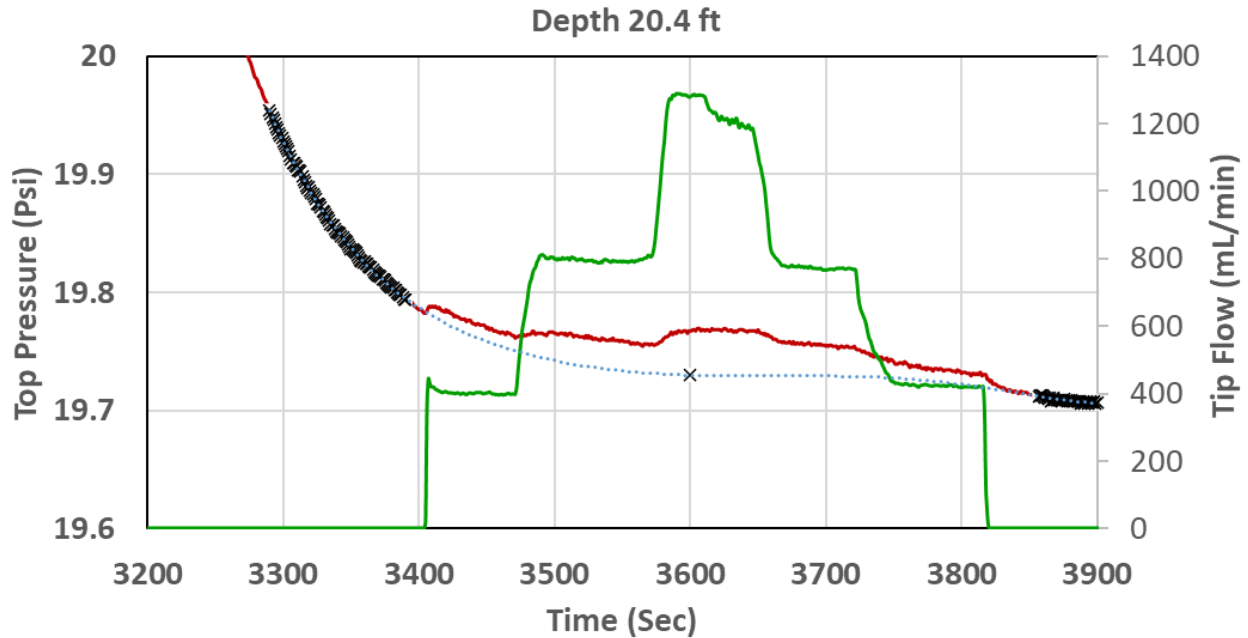


**Figure A6.** Measured pressure at the upper transducer port (solid red line) and estimated background pressure trend (dotted line) for the DPP test at a depth of 20.4 ft in HRK1. The green line is the flow injection rate during the DPP test. The difference between the measured and

background pressure lines is considered to be the injection-induced response used in K estimation.

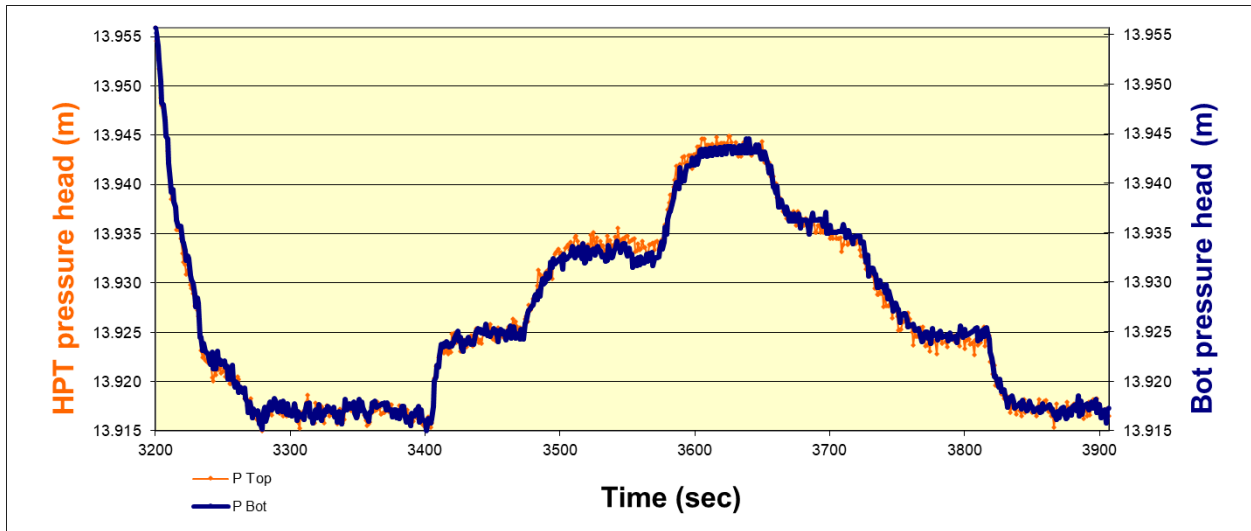
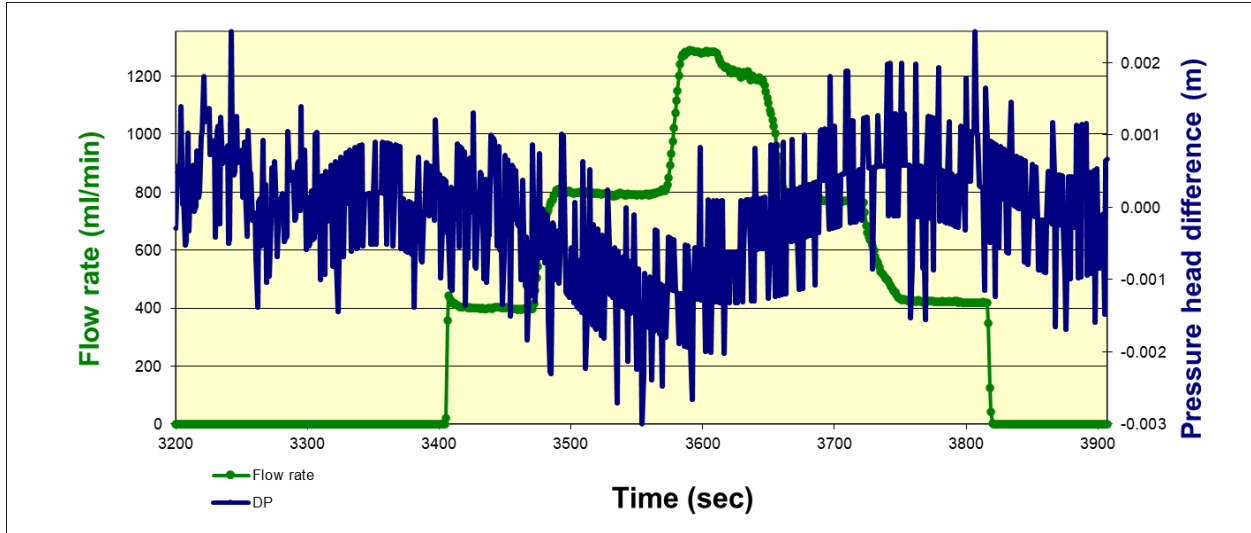


**Figure A7.** Flow rate and pressure difference between the upper and lower transducer ports (top graph) and background trend-removed pressures at the individual transducer ports (bottom graph) for the DPP test at a depth of 20.4 ft in HRK1. Note that both transducers responded very similarly to tip injection, and the system noise caused small negative pressure differences during portions of the injection test.

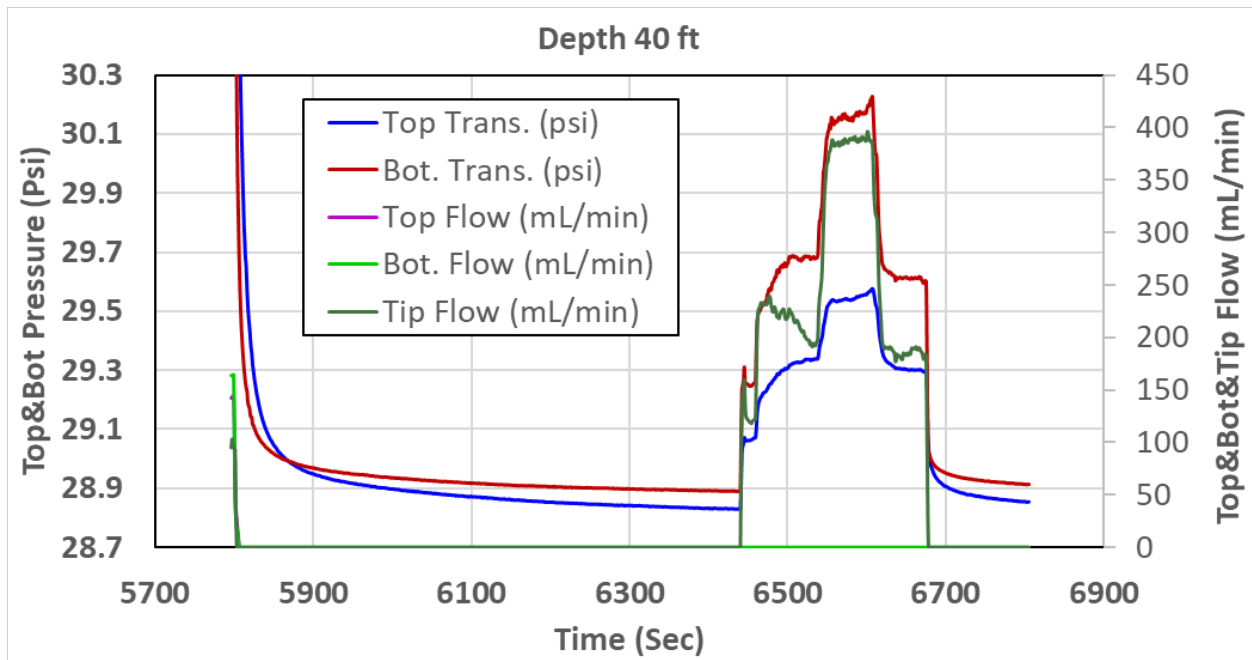


**Figure A8.** Measured pressure at the upper transducer port (Top Trans.) and lower transducer port (Bot. Trans.), flow rate at the upper transducer port (Top Flow) and lower transducer port (Bot. Flow), and flow rate at the tip screen (Tip Flow) before and during the DPP test at a depth of 40 ft in HRK1.

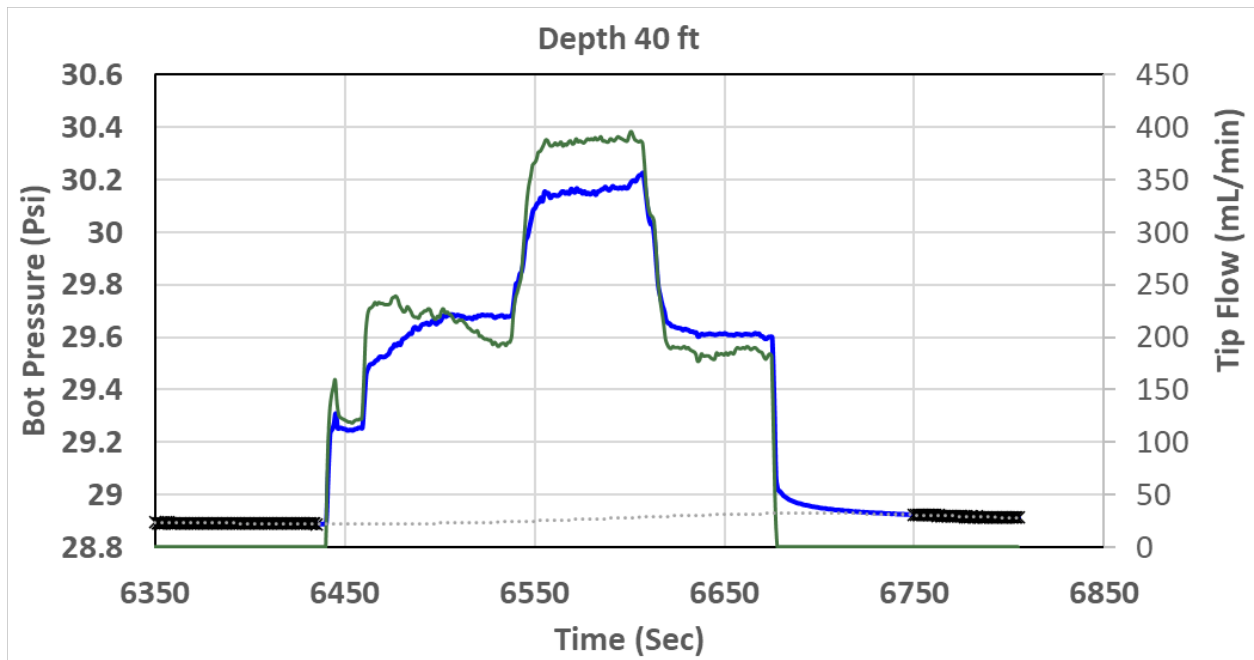


**Figure A9.** Measured pressure at the lower transducer port (solid blue line) and estimated background pressure trend (dotted line) for the DPP test at a depth of 40 ft in HRK1. The green line is the flow injection rate during the DPP test. The difference between the measured and background pressure lines is considered to be the injection-induced response used in K estimation.

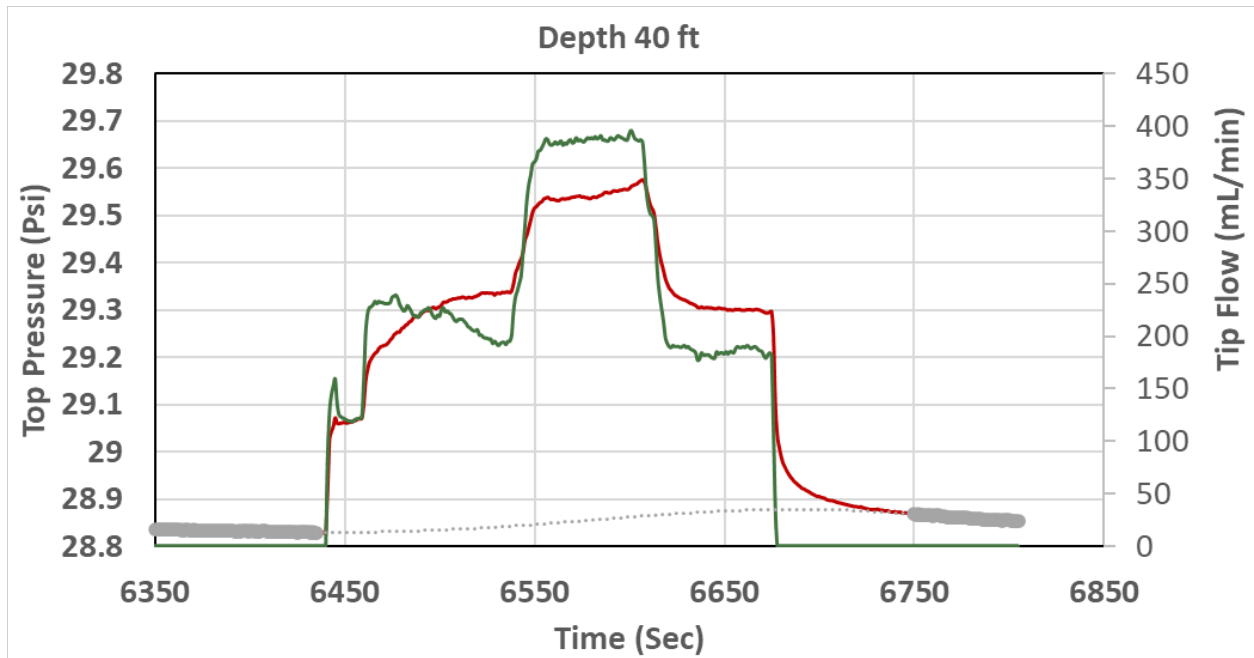


**Figure A10.** Measured pressure at the upper transducer port (solid red line) and estimated background pressure trend (dotted line) for the DPP test at a depth of 40 ft in HRK1. The green line is the flow injection rate during the DPP test. The difference between the measured and

background pressure lines is considered to be the injection-induced response used in K estimation.

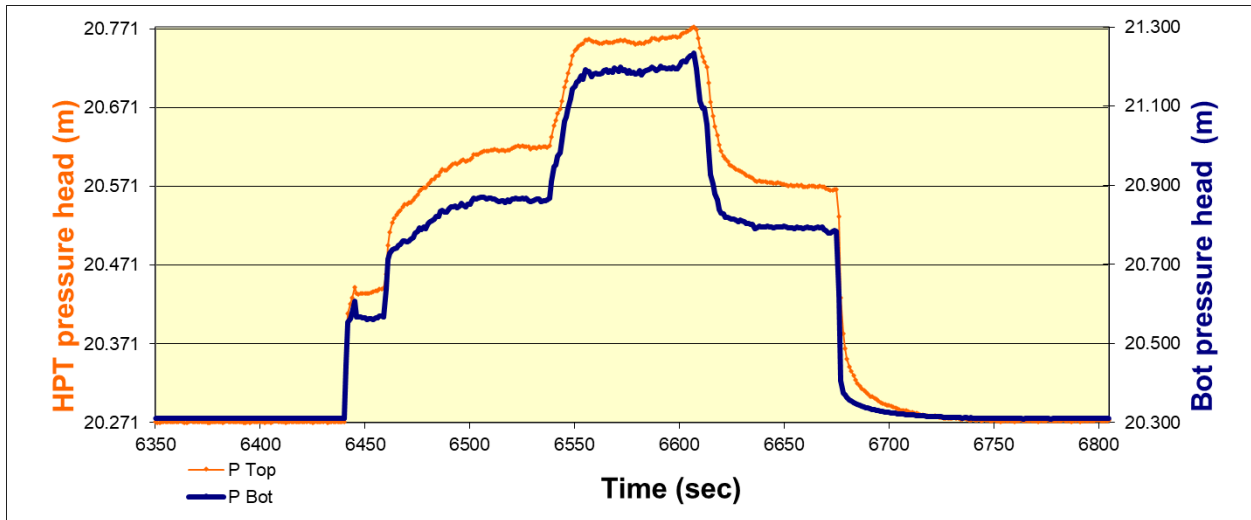
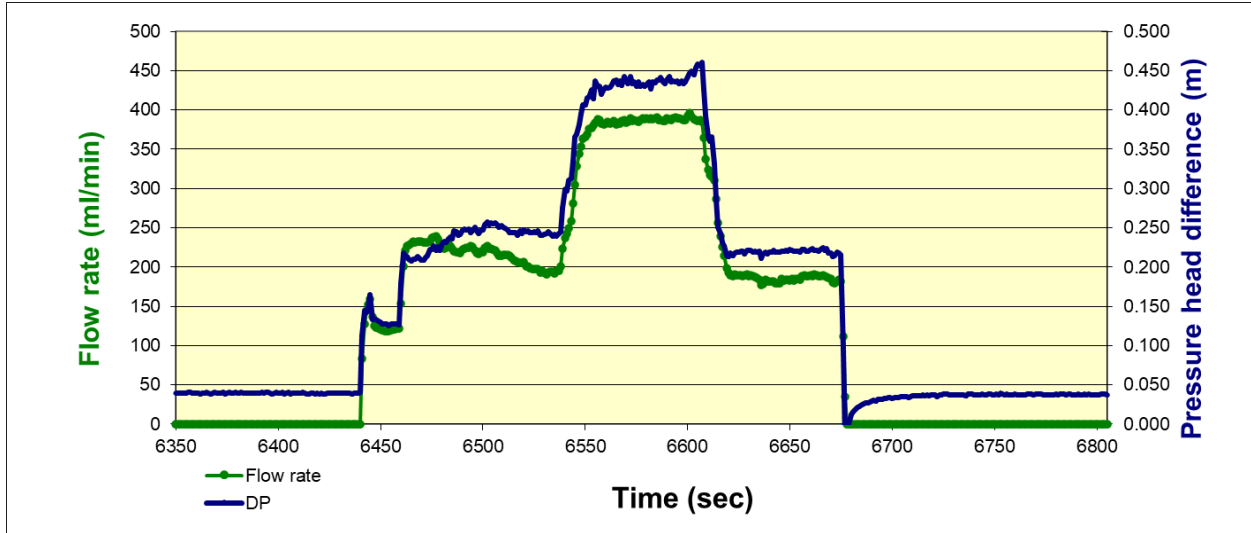


**Figure A11.** Flow rate and pressure difference between the upper and lower transducer ports (top graph) and background trend-removed pressures at the individual transducer ports (bottom graph) for the DPP test at a depth of 40 ft in HRK1.

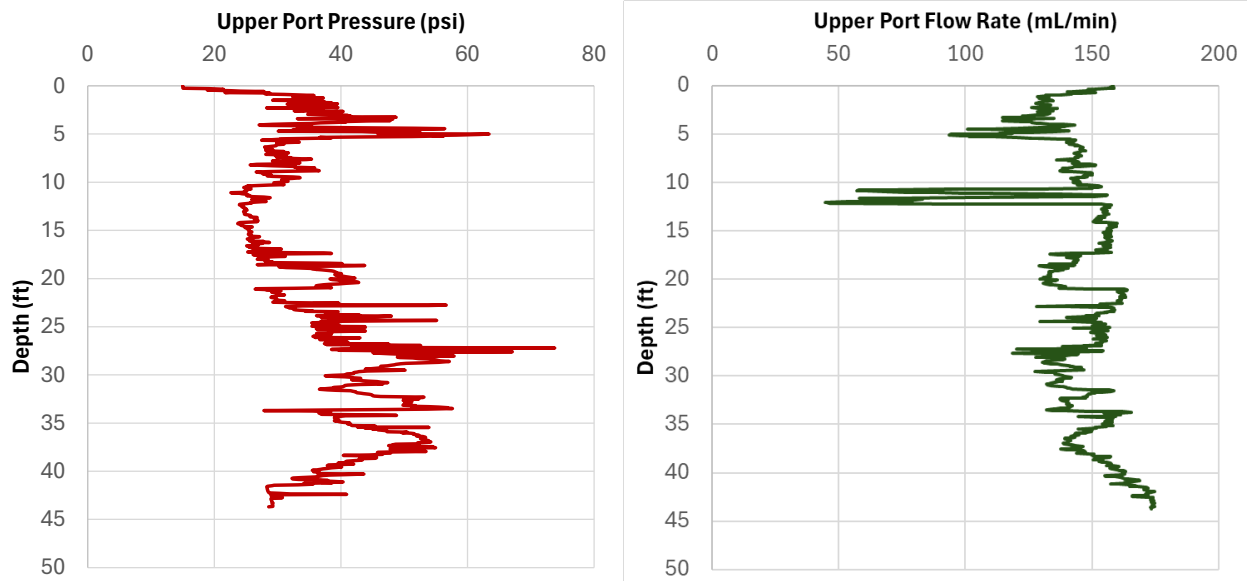


**Figure A12.** Measured pressure (left) and injection rate (right) at the upper transducer port during HRK2 continuous profiling.

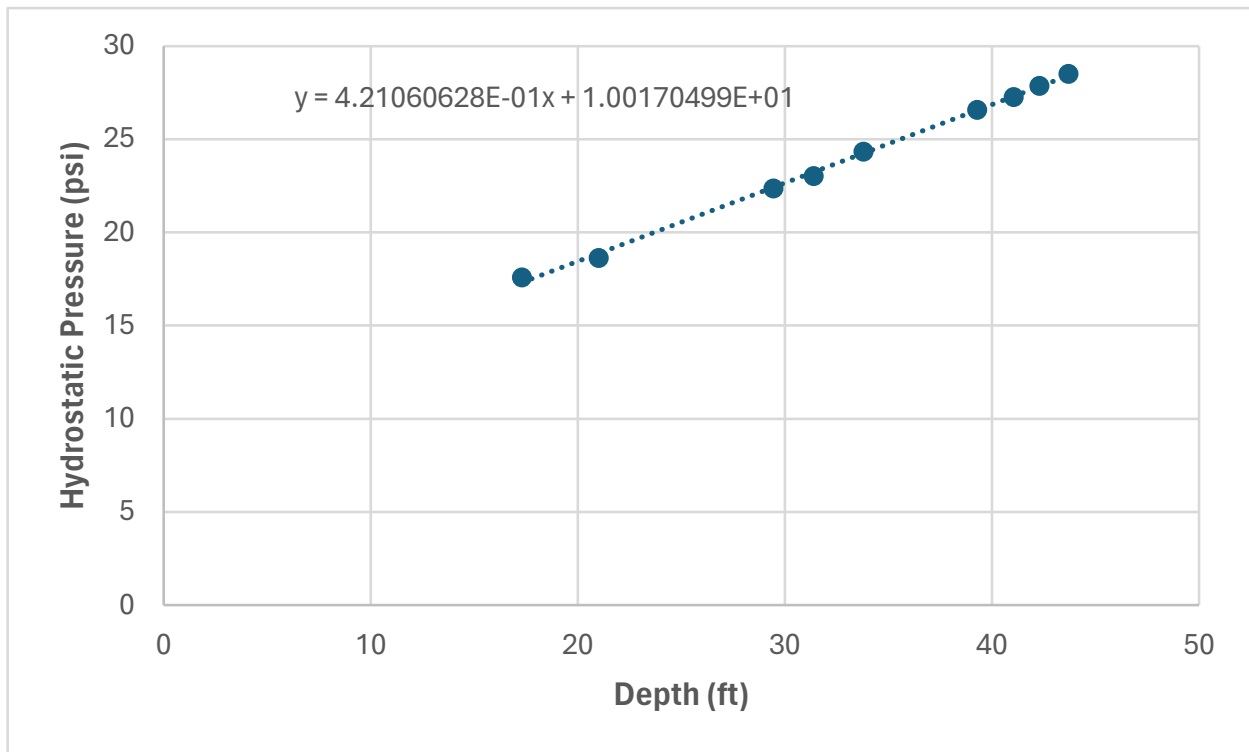


**Figure A13.** Hydrostatic pressure line for the HRK2 depth profile. The depth to the water table is estimated to be 10.5 ft. The equation of the fitted line is used for computing the hydrostatic pressure below the water table (the hydrostatic pressure at the water table is equal to atmospheric pressure).

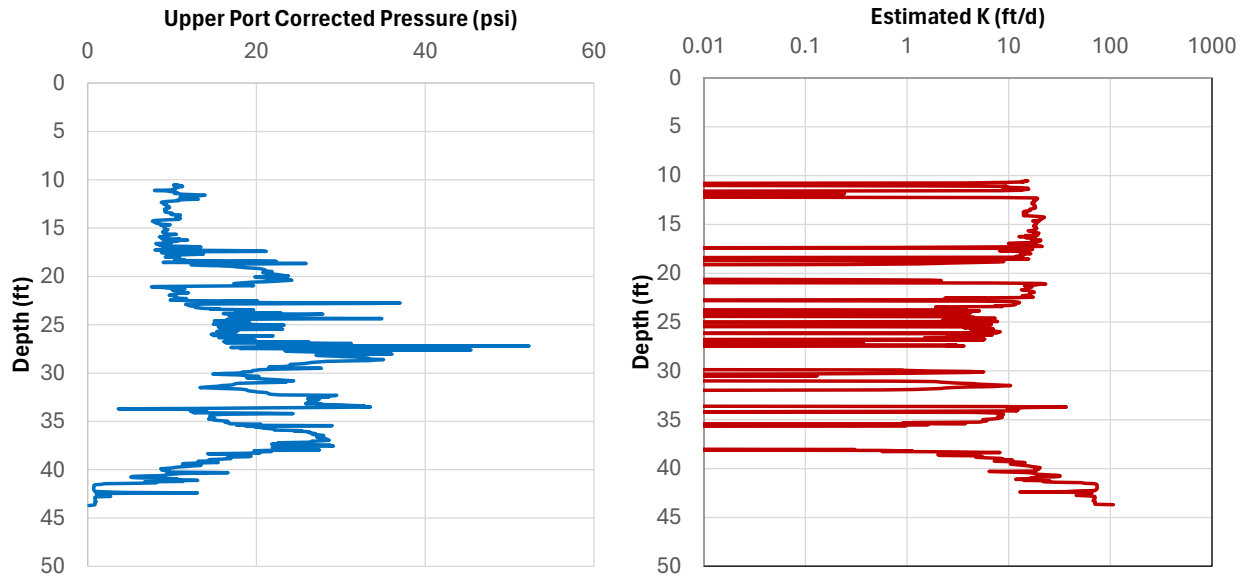


**Figure A14.** Upper transducer port corrected pressure (left) and estimated DPIL K (right) for the HRK2 profile.

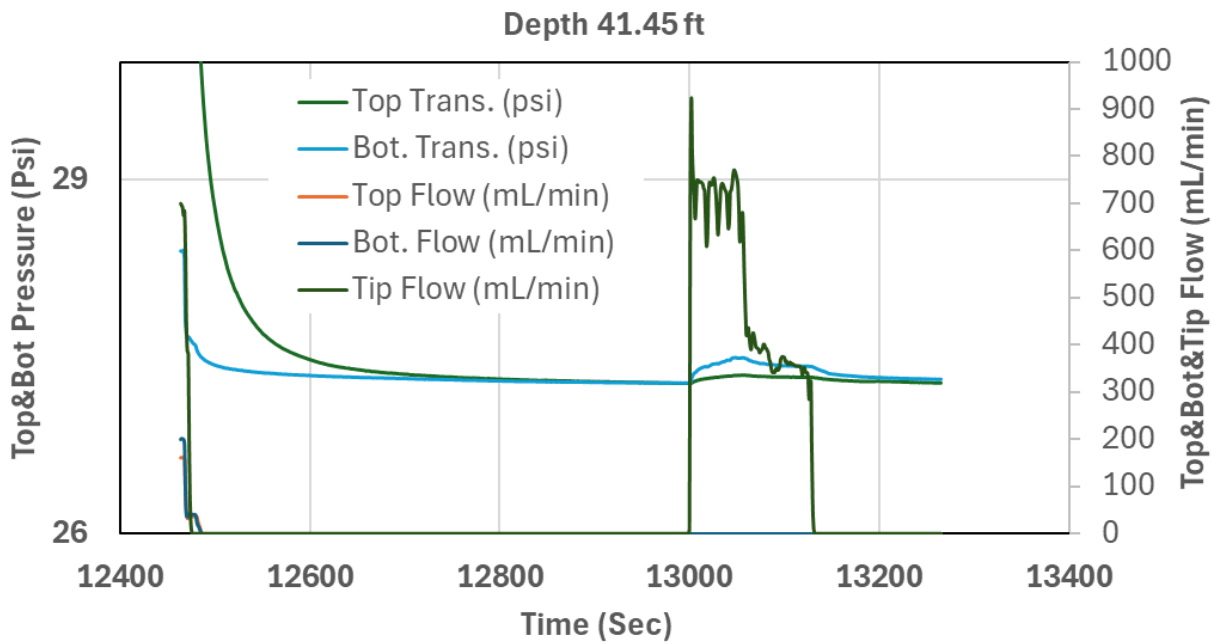


**Figure A15.** Measured pressure at the upper transducer port (Top Trans.) and lower transducer port (Bot. Trans.), flow rate at the upper transducer port (Top Flow) and lower transducer port (Bot. Flow), and flow rate at the tip screen (Tip Flow) before and during the DPP test at a depth of 41.45 ft in HRK2.

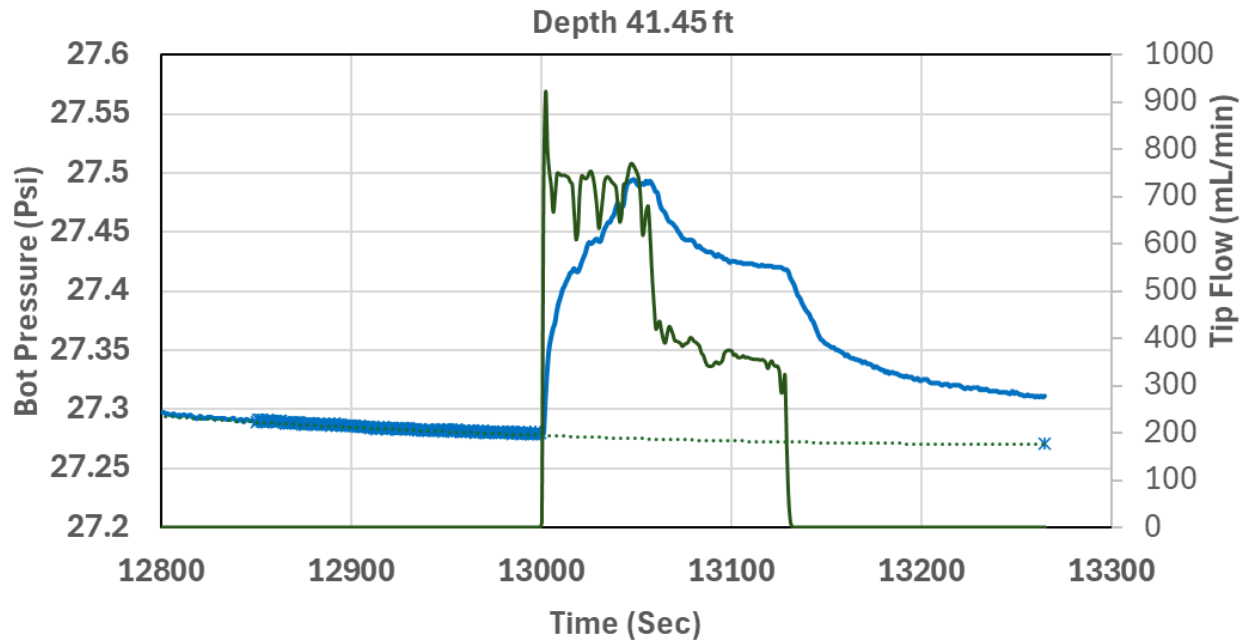


**Figure A16.** Measured pressure at the lower transducer port (solid blue line) and estimated background pressure trend (dotted line) for the DPP test at a depth of 41.45 ft in HRK2. The green line is the flow injection rate during the DPP test. The difference between the measured and background pressure lines is considered to be the injection-induced pressure response used in K estimation.

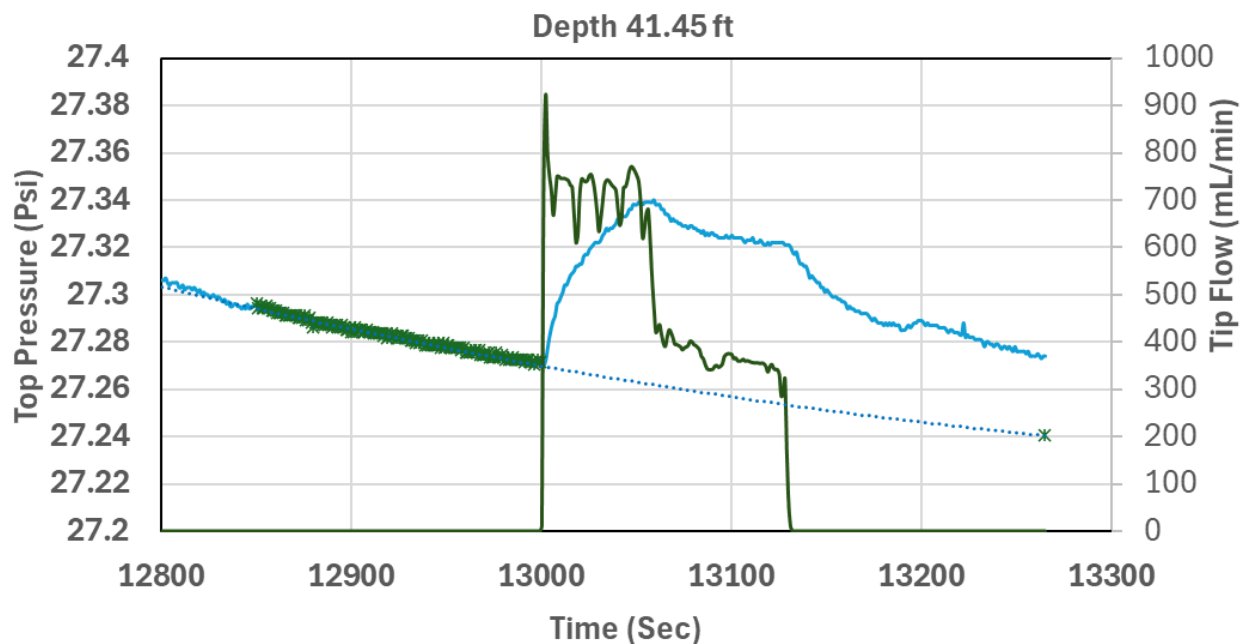


**Figure A17.** Measured pressure at the upper transducer port (solid blue line) and estimated background pressure trend (dotted line) for the DPP test at a depth of 41.45 ft in HRK2. The green line is the flow injection rate during the DPP test. The difference between the measured

and background pressure lines is considered to be the injection-induced pressure response used in K estimation.

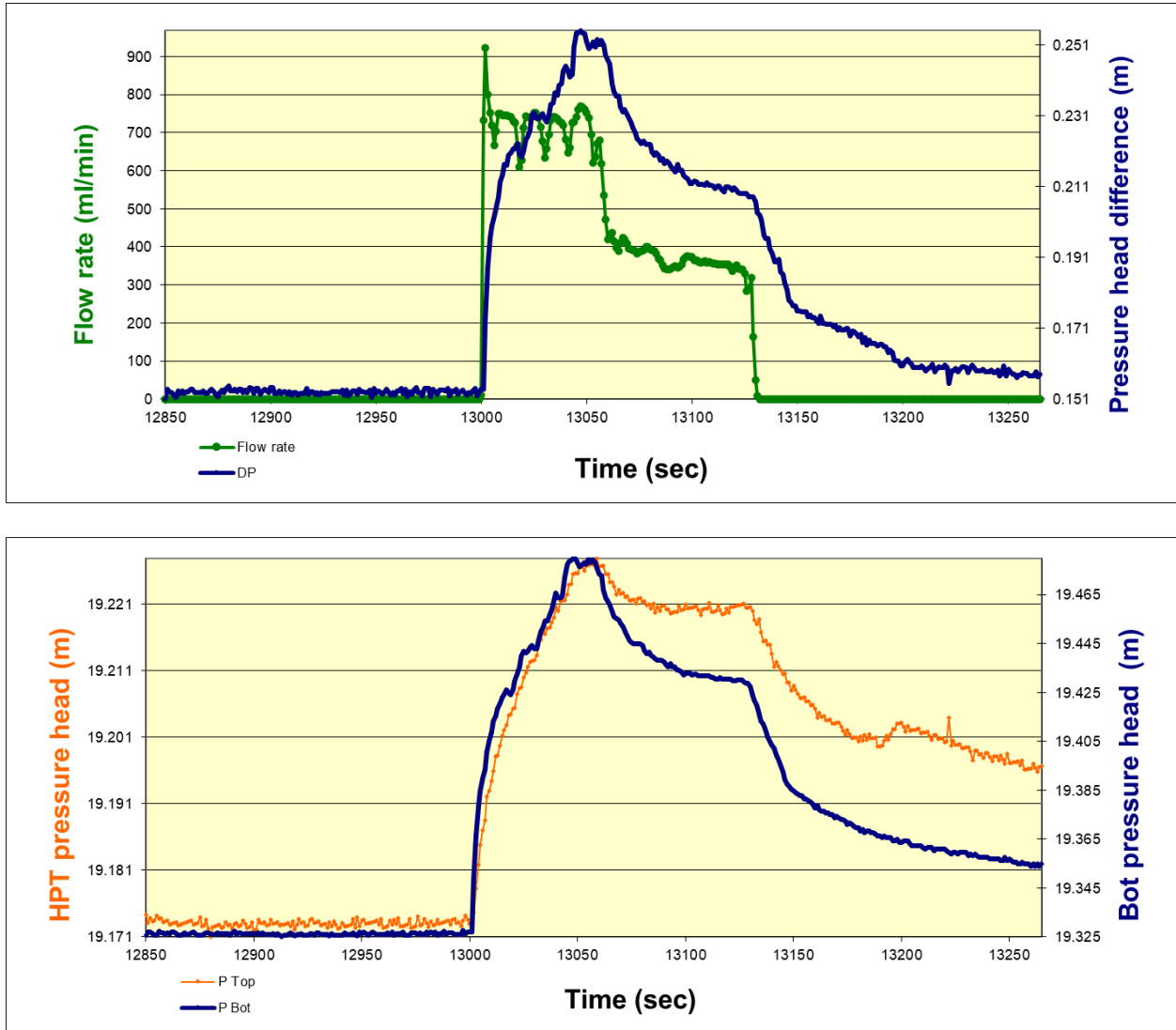


**Figure A18.** Flow rate and pressure difference between the upper and lower transducer ports (top graph) and background trend-removed pressures at the individual transducer ports (bottom graph) for the DPP test at a depth of 41.45 ft in HRK2.

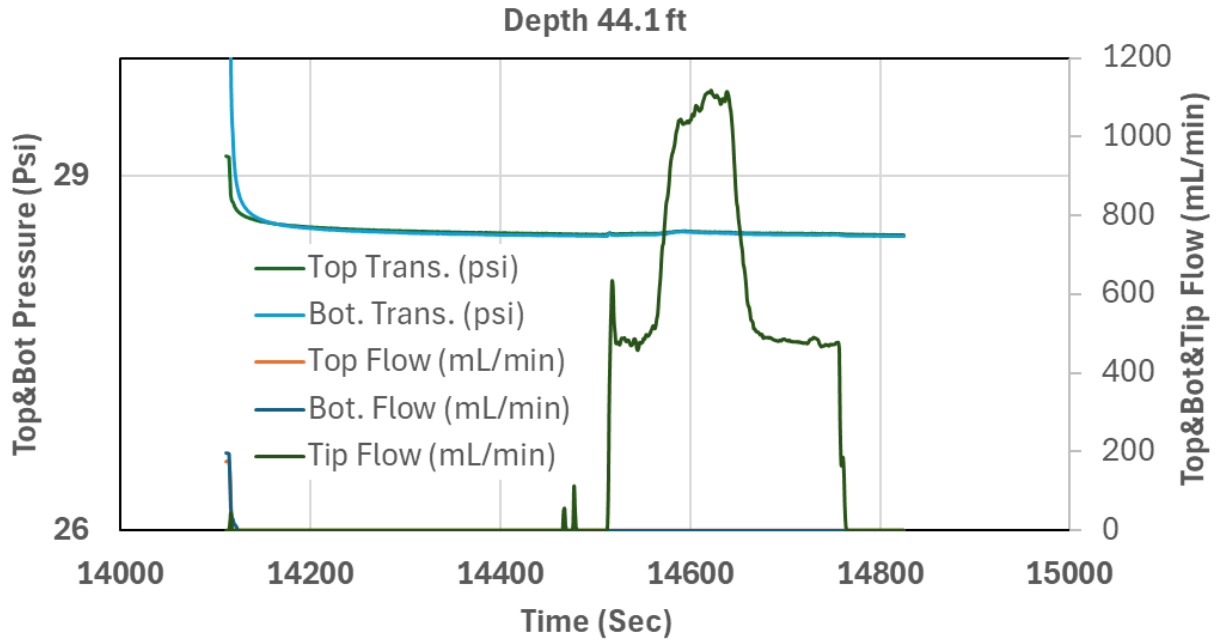


**Figure A19.** Measured pressure at the upper transducer port (Top Trans.) and lower transducer port (Bot. Trans.), flow rate at the upper transducer port (Top Flow) and lower transducer port (Bot. Flow), and flow rate at the tip screen (Tip Flow) before and during the DPP test at a depth of 44.1 ft in HRK2.

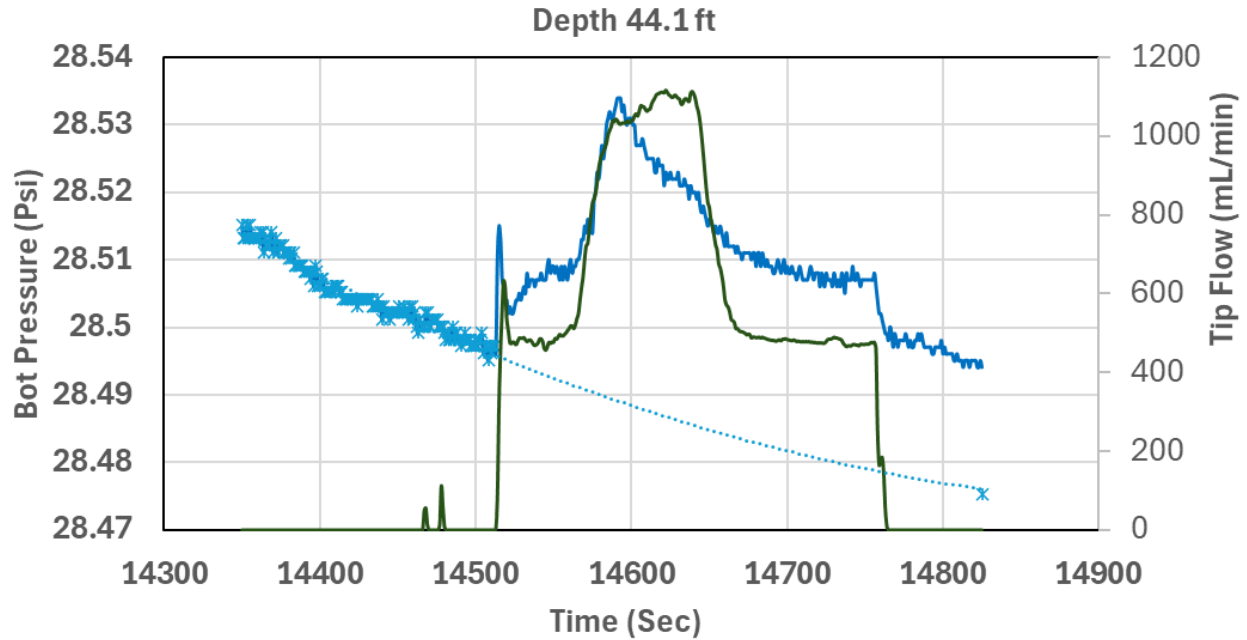


**Figure A20.** Measured pressure at the lower transducer port (solid blue line) and estimated background pressure trend (dotted line) for the DPP test at a depth of 44.1 ft in HRK2. The green line is the flow injection rate during the DPP test. The difference between the measured and background pressure lines is considered to be the injection-induced pressure response used in K estimation.

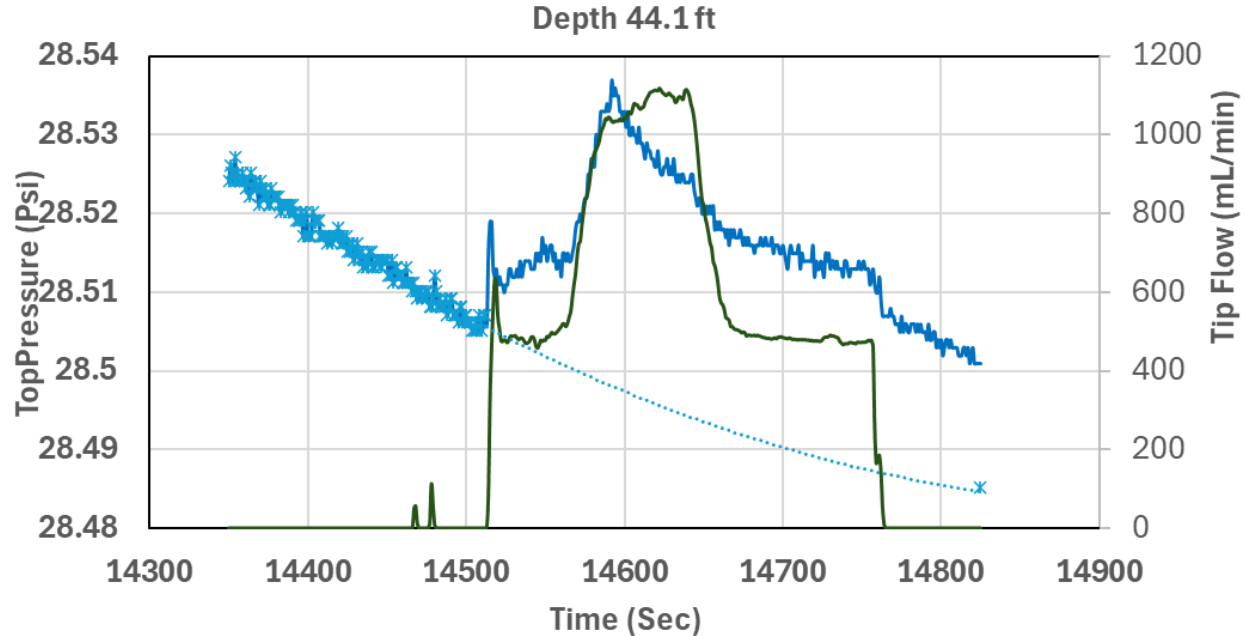


**Figure A21.** Measured pressure at the upper transducer port (solid blue line) and estimated background pressure trend (dotted line) for the DPP test at a depth of 44.1 ft in HRK2. The green line is the flow injection rate during the DPP test. The difference between the measured and

background pressure lines is considered to be the injection-induced pressure response used in K estimation.

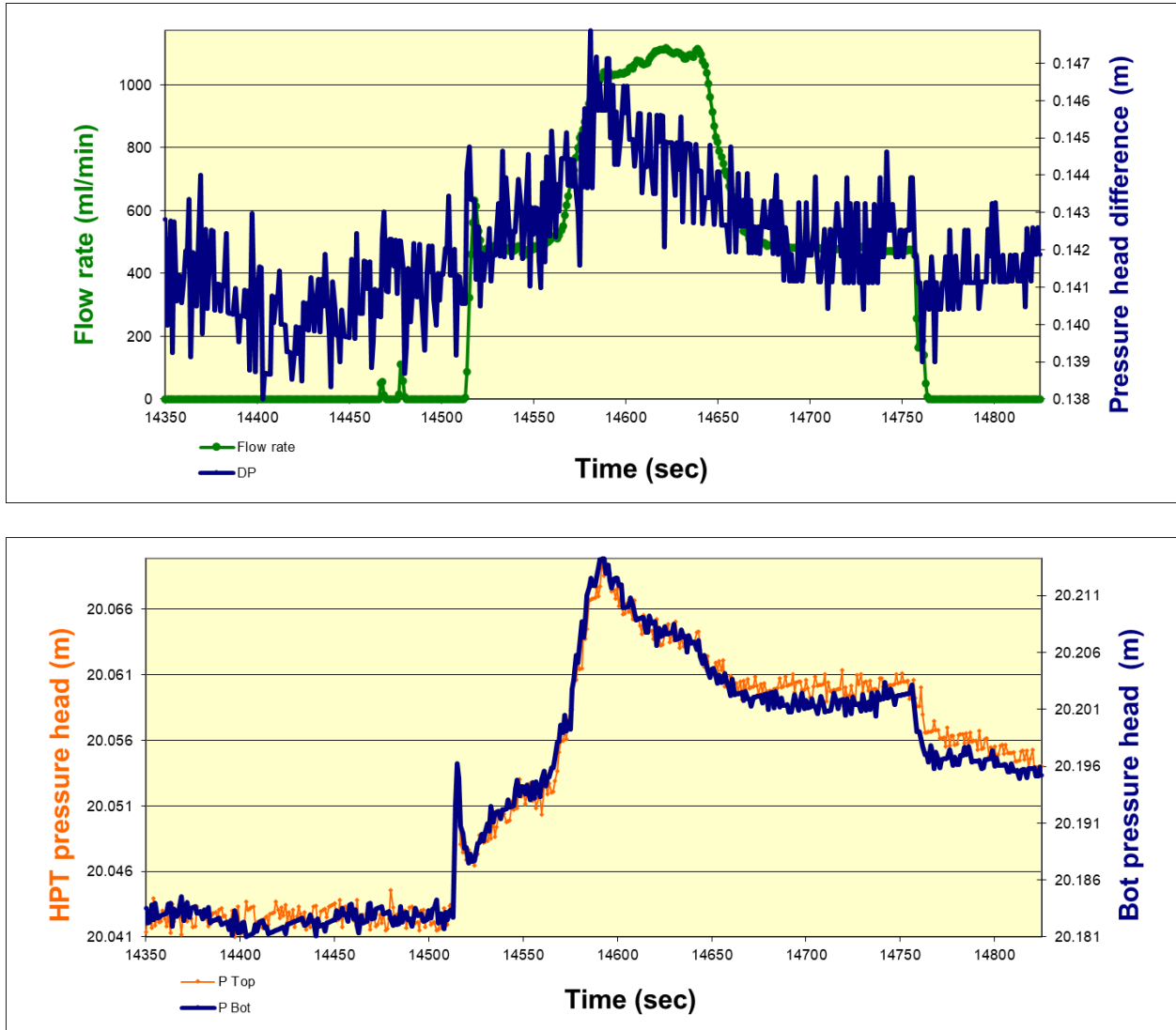


**Figure A22.** Flow rate and pressure difference between the upper and lower transducer ports (top graph) and background trend-removed pressures at the individual transducer ports (bottom graph) for the DPP test at a depth of 44.1 ft in HRK2.

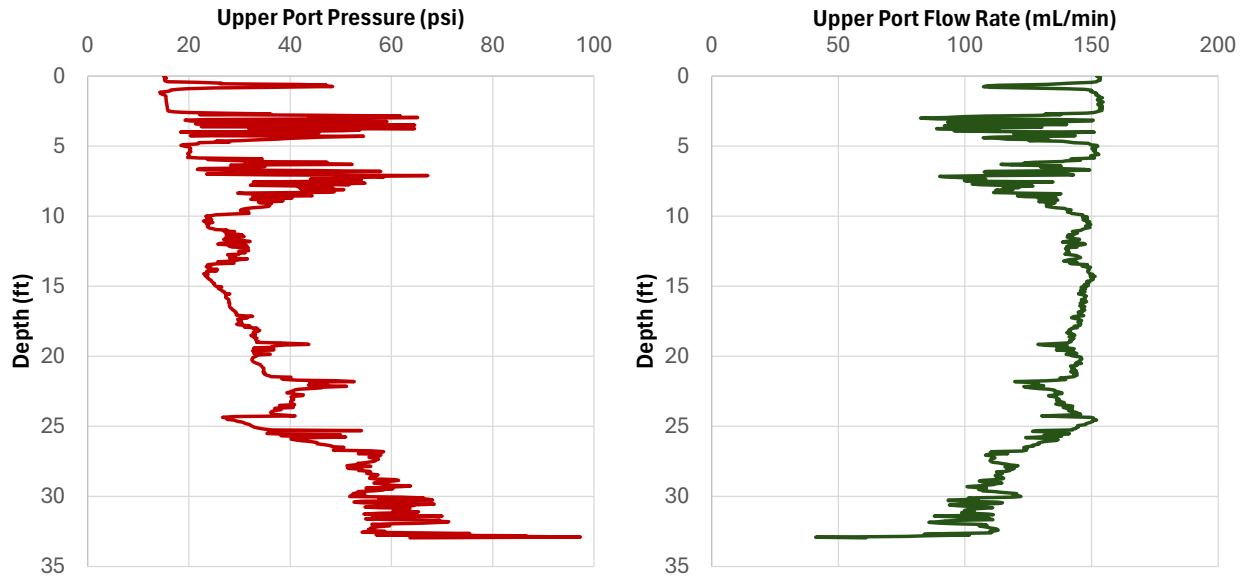


**Figure A23.** Measured pressure (left) and injection rate (right) at the upper transducer port during HRK3 continuous profiling.

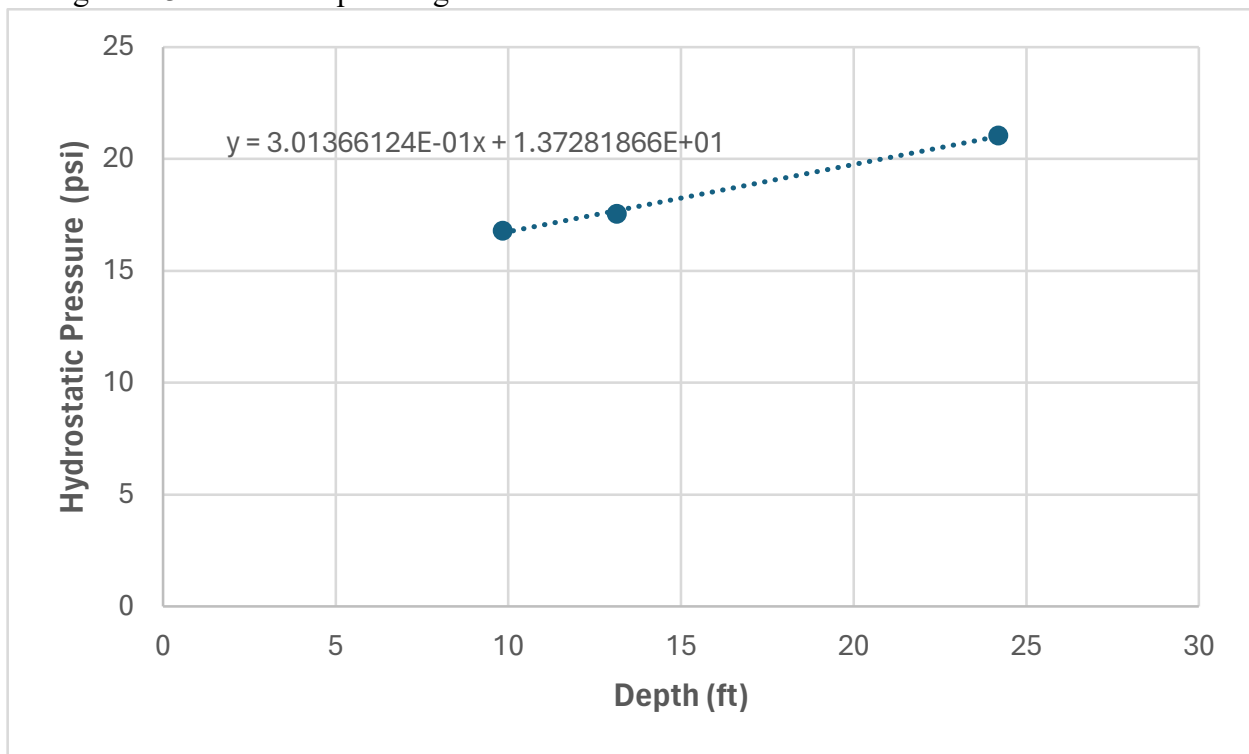


**Figure A24.** Hydrostatic pressure line for the HRK3 depth profile. The depth to the water table is estimated to be 8.25 ft. The equation of the fitted line is used for computing the hydrostatic pressure below the water table (the hydrostatic pressure at the water table is equal to atmospheric pressure).

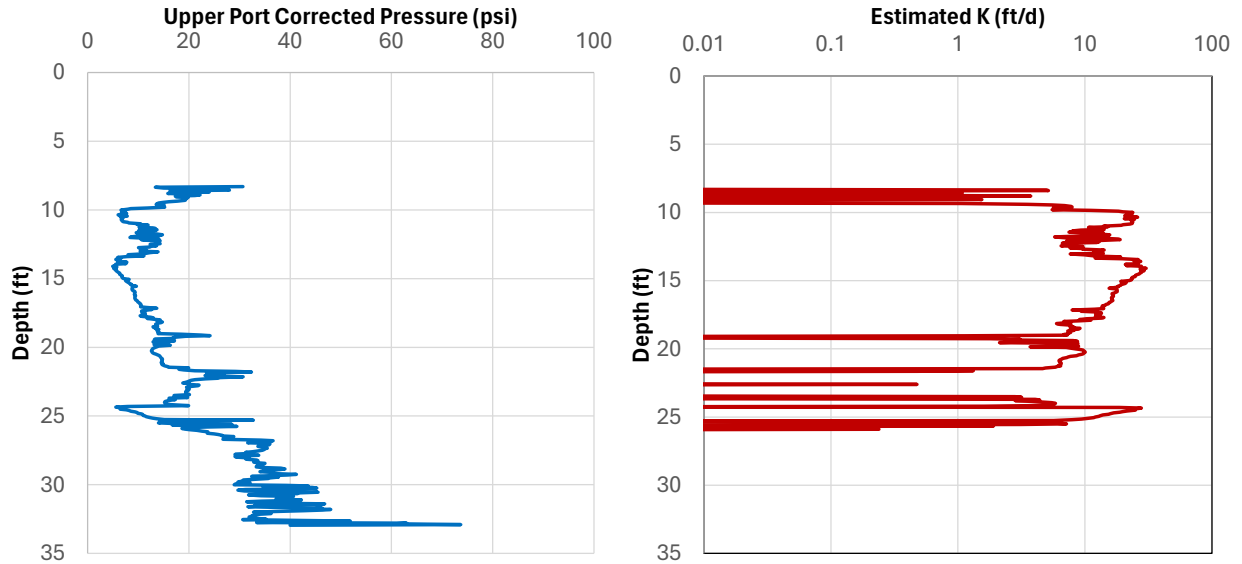


**Figure A25.** Upper transducer port corrected pressure (left) and estimated DPIL K (right) for the HRK3 profile.

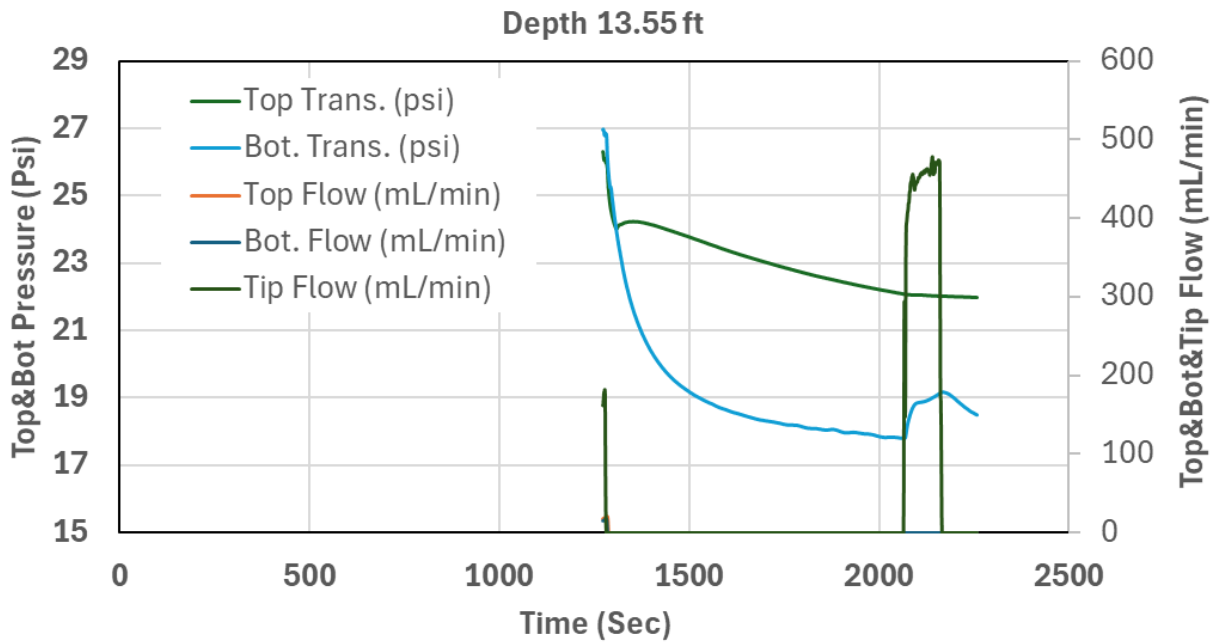


**Figure A26.** Measured pressure at the upper transducer port (Top Trans.) and lower transducer port (Bot. Trans.), flow rate at the upper transducer port (Top Flow) and lower transducer port (Bot. Flow), and flow rate at the tip screen (Tip Flow) before and during the DPP test at a depth of 13.55 ft in HRK3.

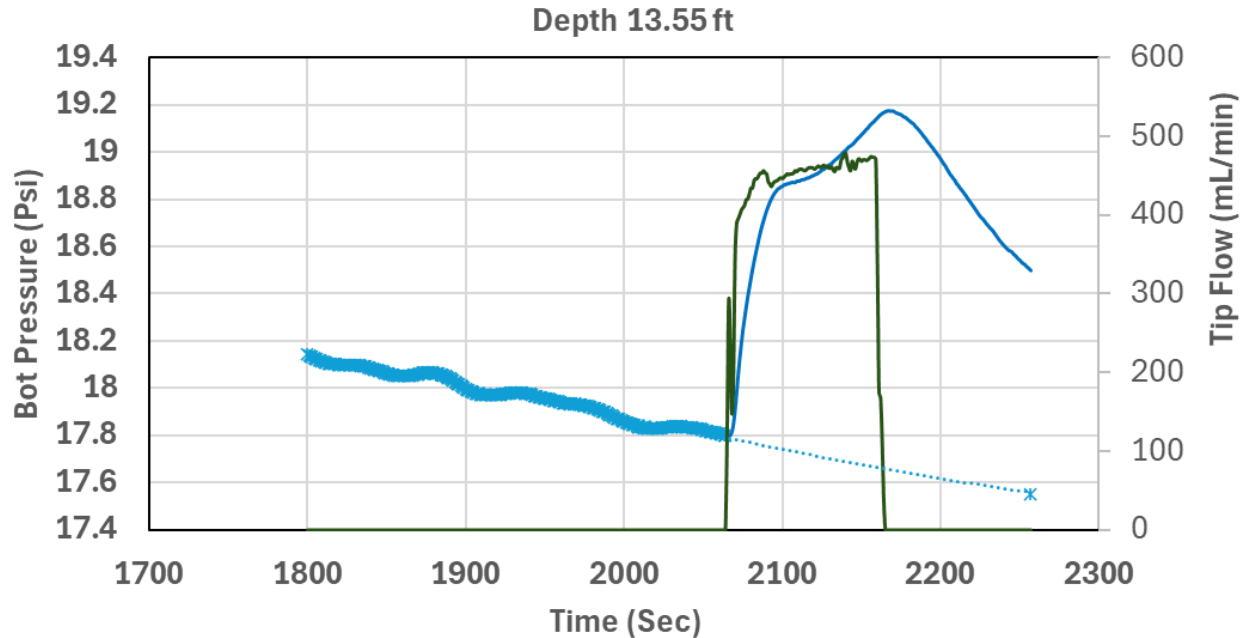


**Figure A27.** Measured pressure at the lower transducer port (solid blue line) and estimated background pressure trend (dotted line) for the DPP test at a depth of 13.55 ft in HRK3. The green line is the flow injection rate during the DPP test. The difference between the measured and background pressure lines is considered to be the injection-induced pressure response used in K estimation.

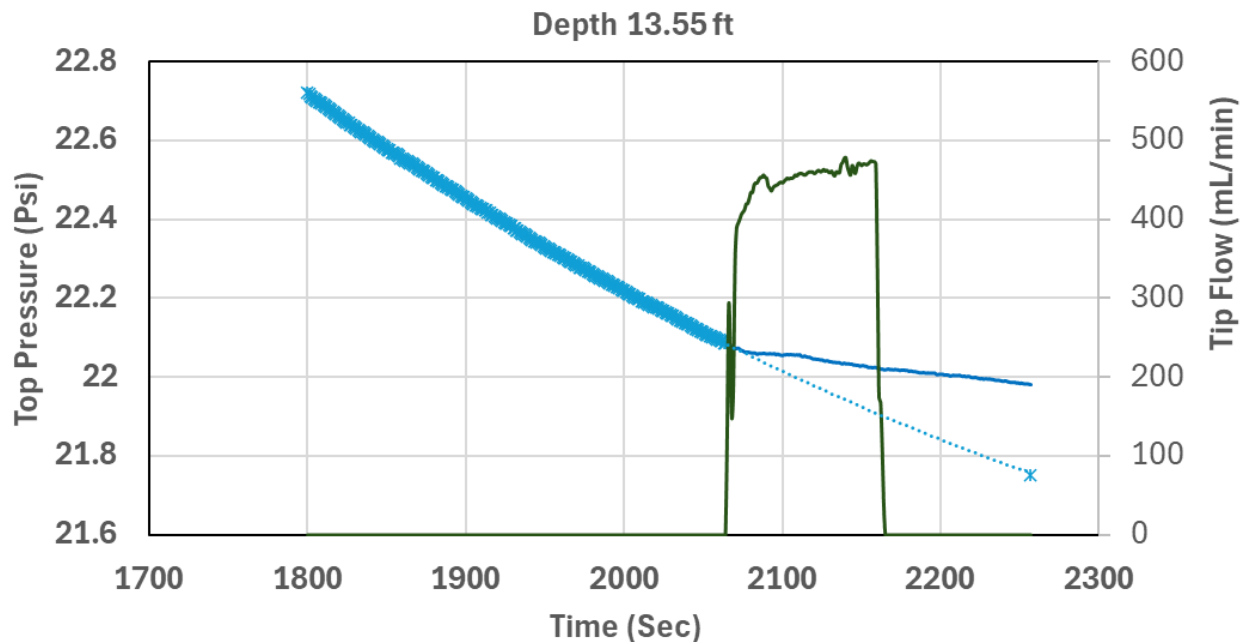


**Figure A28.** Measured pressure at the upper transducer port (solid blue line) and estimated background pressure trend (dotted line) for the DPP test at a depth of 13.55 ft in HRK3. The green line is the flow injection rate during the DPP test. The difference between the measured

and background pressure lines is considered to be the injection-induced pressure response used in K estimation.

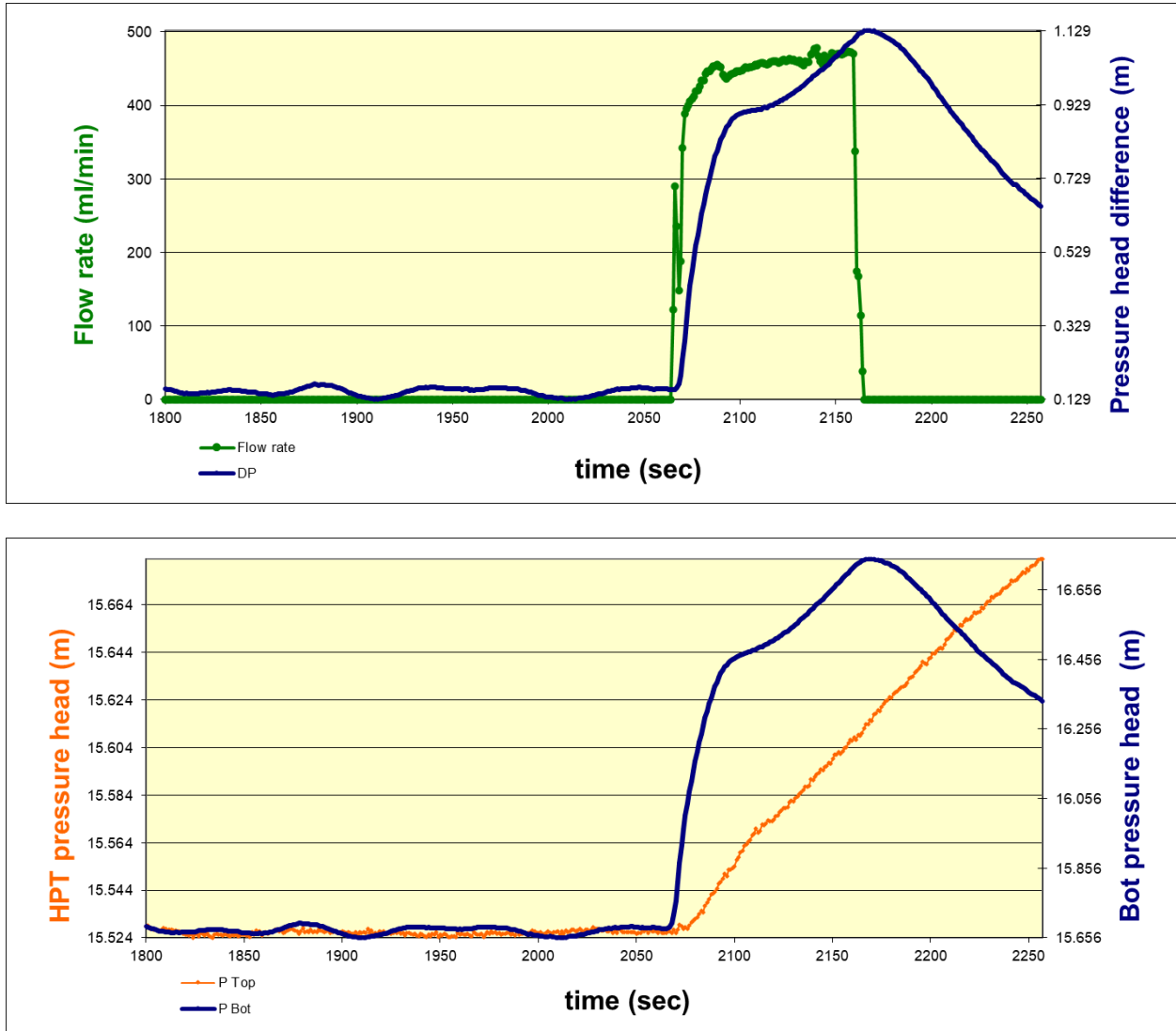


**Figure A29.** Flow rate and pressure difference between the upper and lower transducer ports (top graph) and background trend-removed pressures at the individual transducer ports (bottom graph) for the DPP test at a depth of 13.55 ft in HRK3.

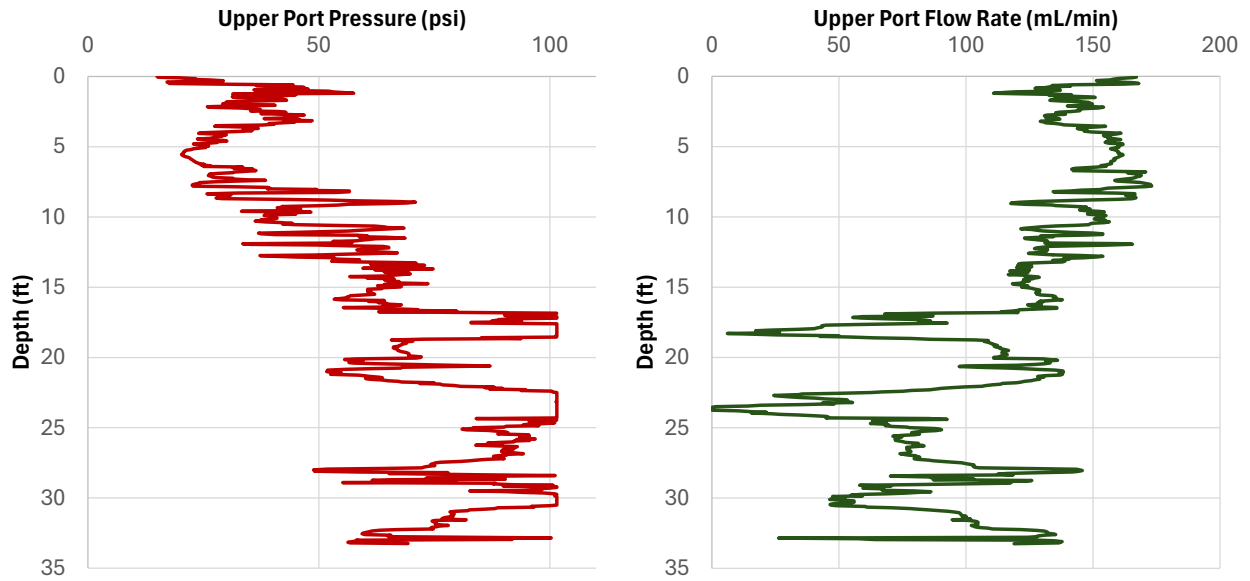


**Figure A30.** Measured pressure (left) and injection rate (right) at the upper transducer port during HRK4 continuous profiling.

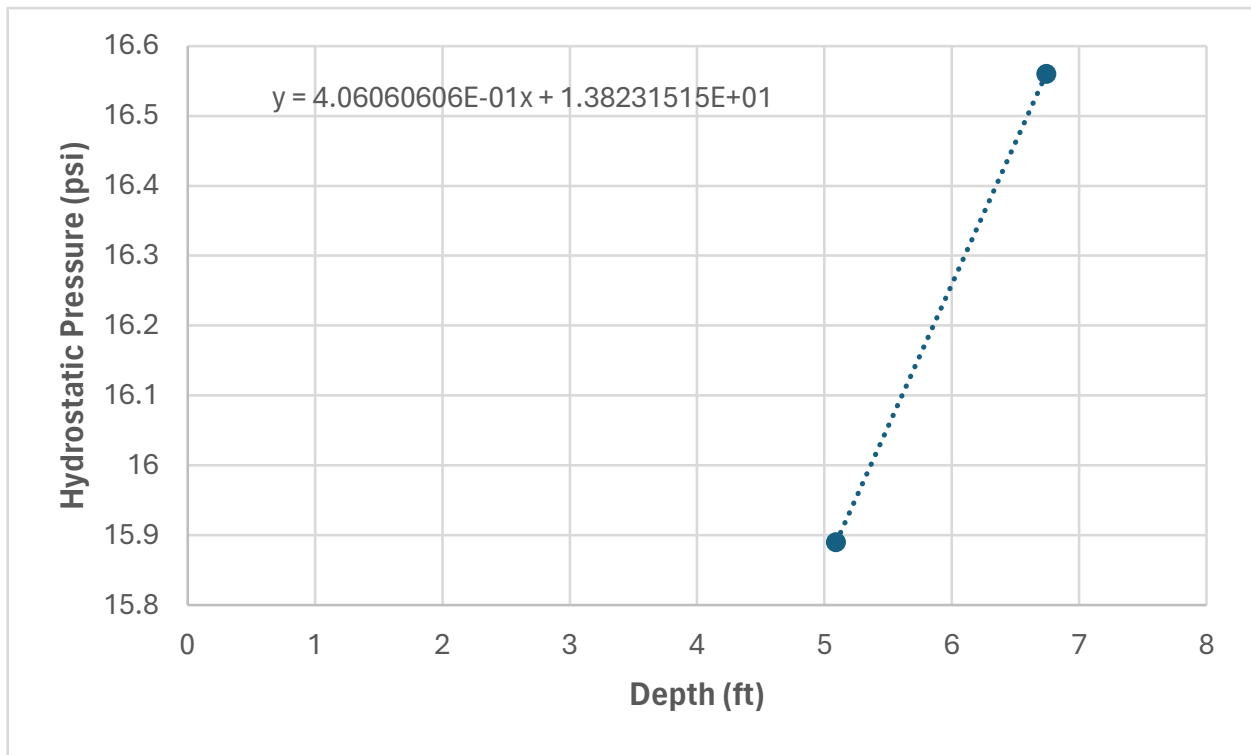


**Figure A31.** Hydrostatic pressure line for the HRK4 depth profile. The depth to the water table is estimated to be 4.25 ft. The equation of the fitted line is used for computing the hydrostatic pressure below the water table (the hydrostatic pressure at the water table is equal to atmospheric pressure).

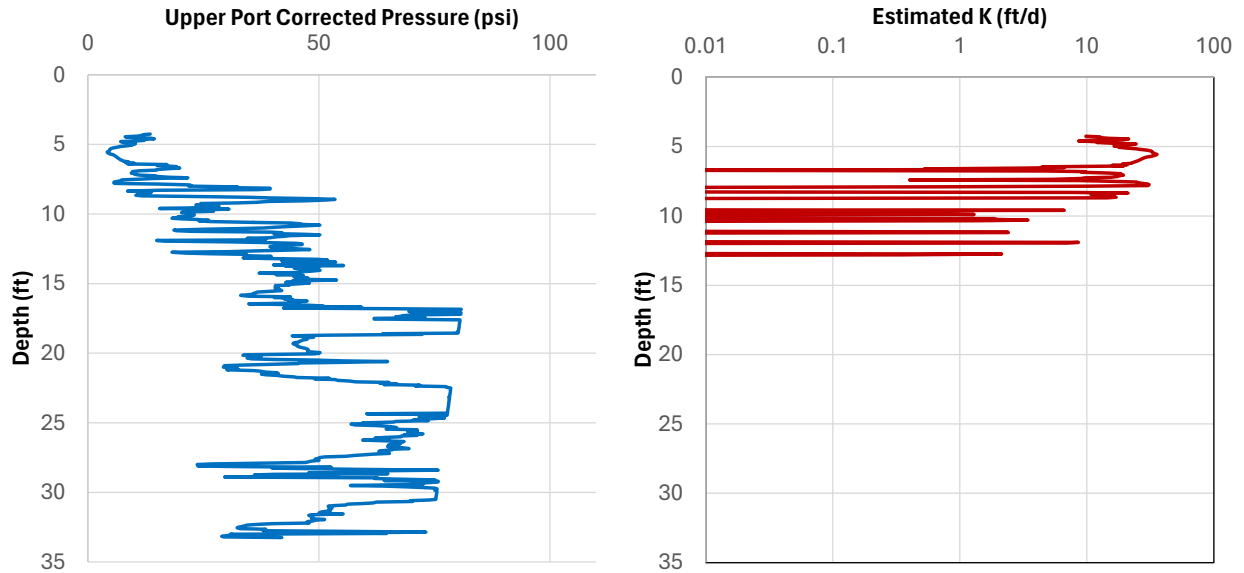


**Figure A32.** Upper transducer port corrected pressure (left) and estimated DPIL K (right) for the HRK4 profile.

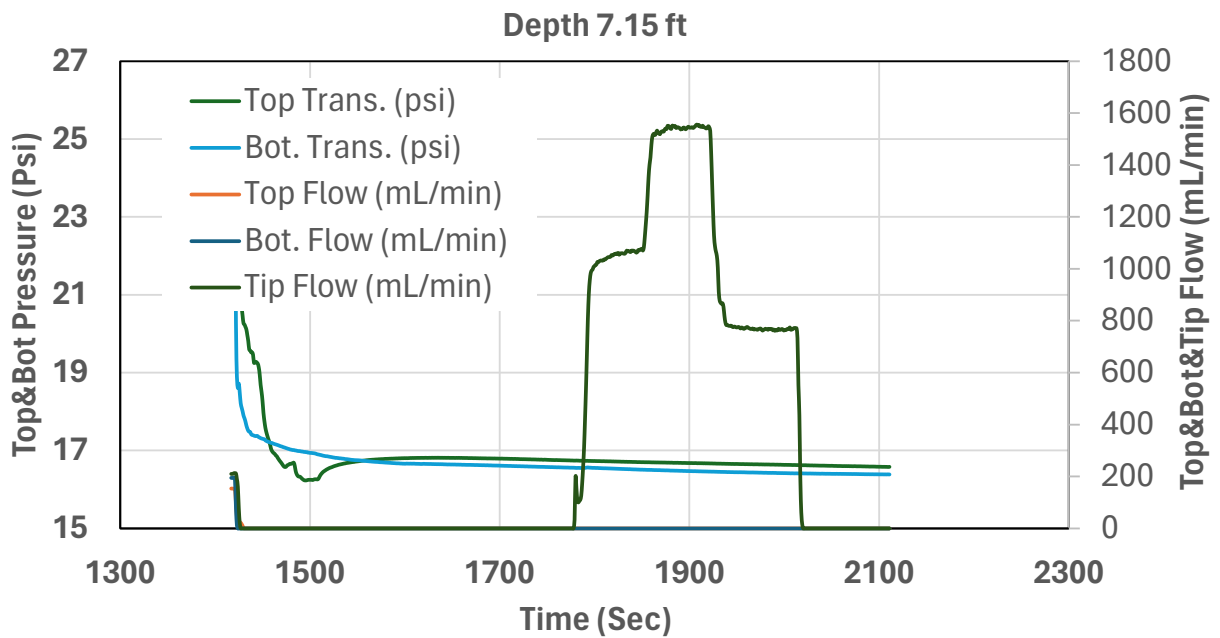


**Figure A33.** Measured pressure at the upper transducer port (Top Trans.) and lower transducer port (Bot. Trans.), flow rate at the upper transducer port (Top Flow) and lower transducer port (Bot. Flow), and flow rate at the tip screen (Tip Flow) before and during the DPP test at a depth of 7.15 ft in HRK4.

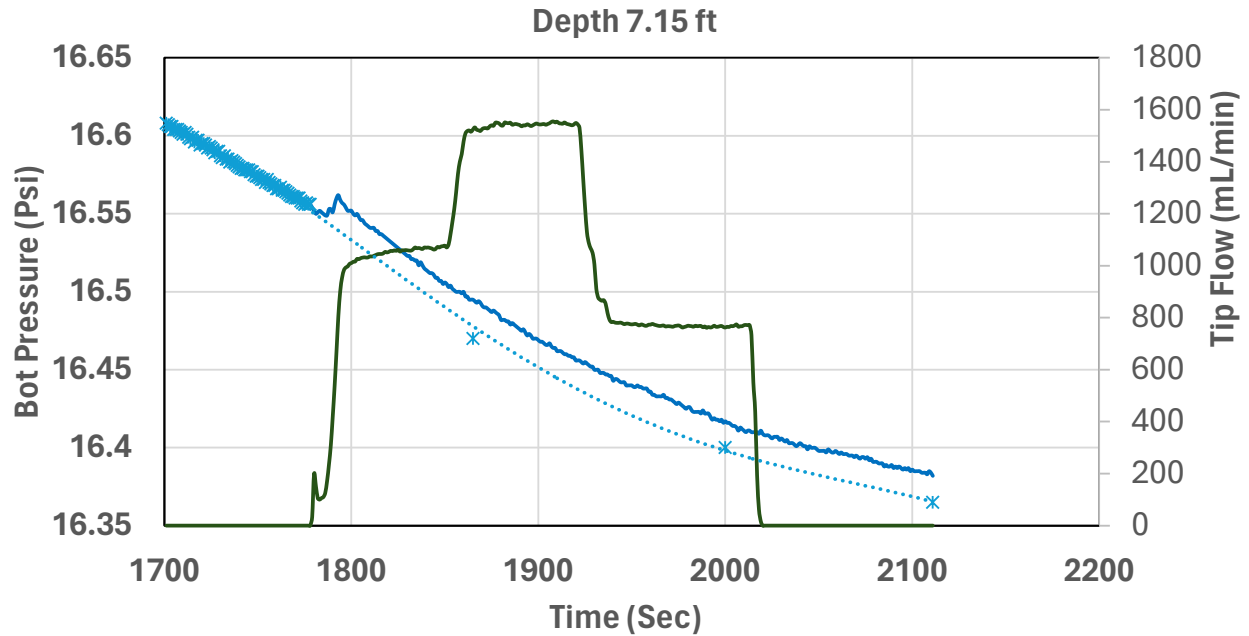


**Figure A34.** Measured pressure at the lower transducer port (solid blue line) and estimated background pressure trend (dotted line) for the DPP test at a depth of 7.15 ft in HRK4. The green line is the flow injection rate during the DPP test. The difference between the measured and background pressure lines is considered to be the injection-induced pressure response used in K estimation.

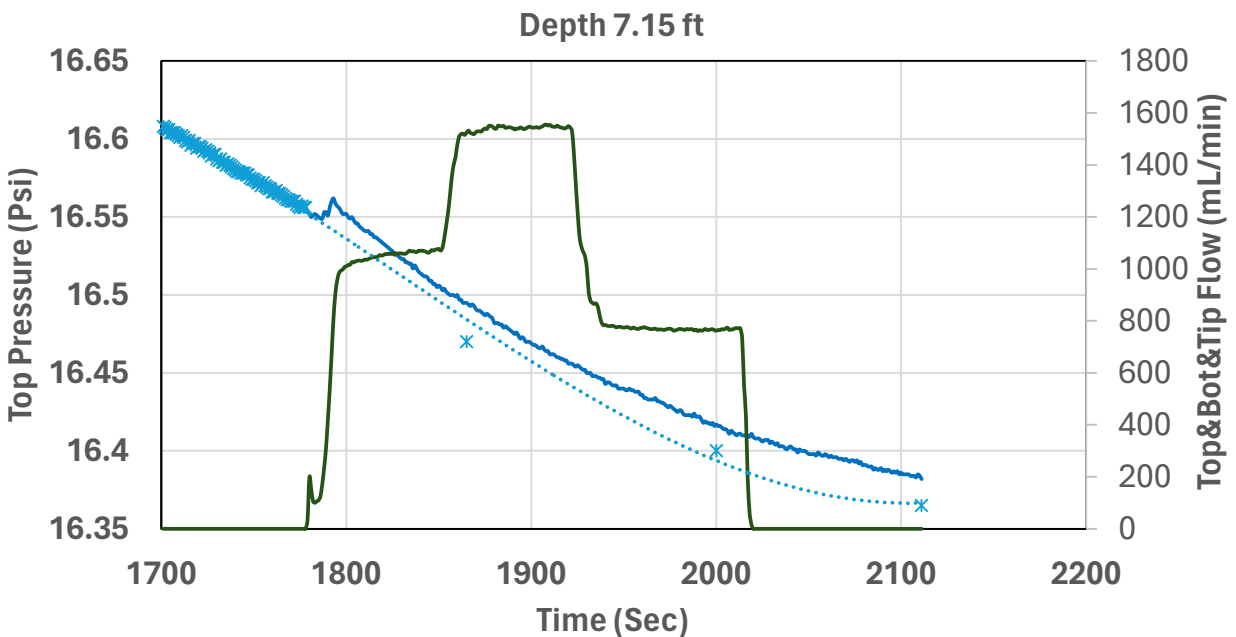


**Figure A35.** Measured pressure at the upper transducer port (solid blue line) and estimated background pressure trend (dotted line) for the DPP test at a depth of 7.15 ft in HRK4. The green line is the flow injection rate during the DPP test. The difference between the measured and background pressure lines is considered to be the injection-induced pressure response used in K estimation.

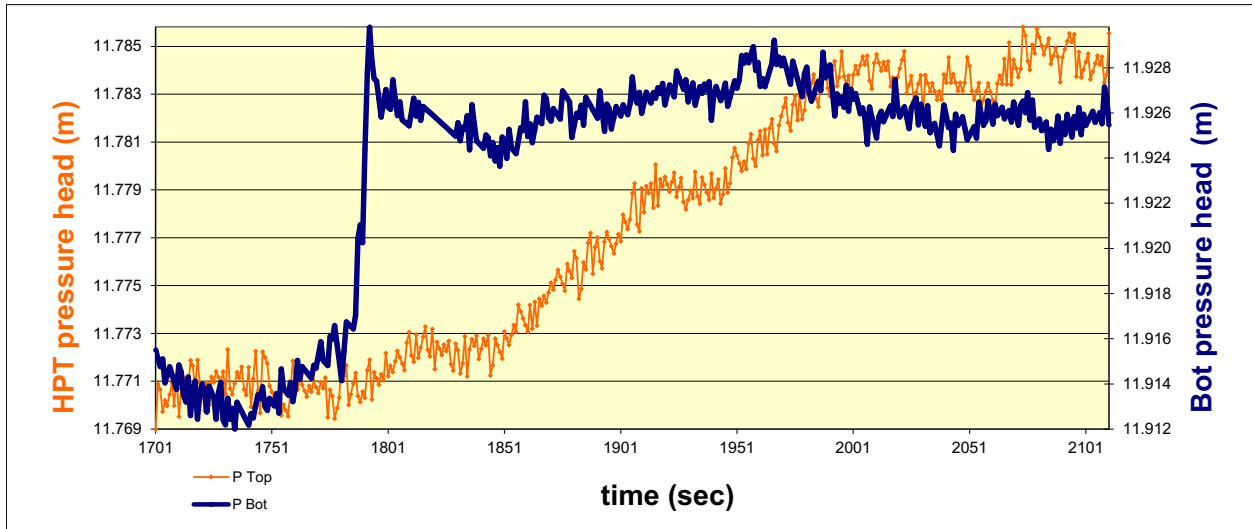
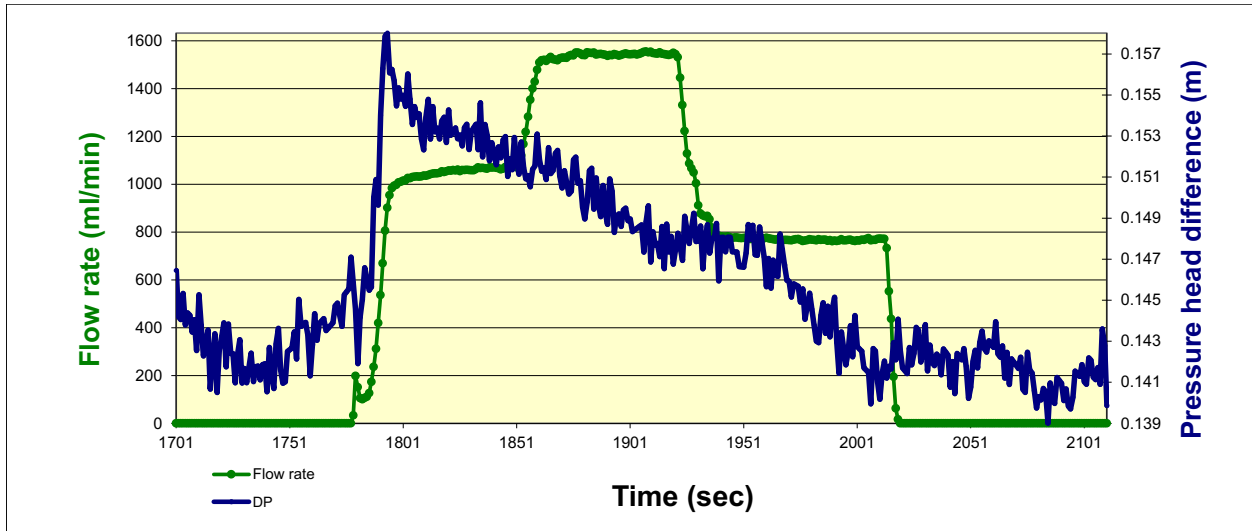


**Figure A36.** Flow rate and pressure difference between the upper and lower transducer ports (top graph) and background trend-removed pressures at the individual transducer ports (bottom graph) for the DPP test at a depth of 7.15 ft in HRK4.

## REFERENCES

- American Society of Testing and Materials (ASTM), 2016, Standard practice for direct push hydraulic logging for profiling variations of permeability in soils. D8037: West Conshohocken, Pennsylvania, ASTM International. [www.astm.org](http://www.astm.org).
- Butler, J. J., Jr., Dietrich, P., Wittig, V., and Christy, T., 2007, Characterizing hydraulic conductivity with the direct-push permeameter: *Groundwater*, v. 45, no. 4, p. 409–419, doi:10.1111/j.1745-6584.2007.00300.x.
- Dietrich, P., Butler, J. J., Jr., and Faiss, K., 2008, A rapid method for hydraulic profiling in unconsolidated formations: *Ground Water*, v. 46, no. 2, p. 323–328, doi:10.1111/j.1745-6584.2007.00377.x.
- Geoprobe Systems, 2007, Geoprobe Hydraulic Profiling Tool (HPT) system: Standard operating procedure, Technical Bulletin No. MK3137: Salina, Kansas, Kejr Inc.
- Geoprobe Systems, 2010, Tech guide for calculation of estimated hydraulic conductivity (Est. K) log from HPT Data. Salina, Kansas, Kejr Inc.
- Liu, G., Borden, R., and Butler, J. J., Jr., 2019, Simulation assessment of direct push injection logging for high resolution aquifer characterization: *Groundwater*, v. 57, no. 4, p. 562–574, doi: 10.1111/gwat.12826.
- Liu, G., Bohling, G. C., and Butler Jr., J. J., 2008, Simulation assessment of the direct-push permeameter for characterizing vertical variations in hydraulic conductivity: *Water Resources Research*, 44, W02432, doi:10.1029/2007WR006078.
- Liu, G., Butler, J. J., Jr, Bohling, G. C., Reboulet, E., Knobbe, S., and Hyndman, D. W., 2009, A new method for high-resolution characterization of hydraulic conductivity: *Water Resources Research*, v. 45, W08202, doi:10.1029/2009WR008319.
- Maliva, R.G., 2016, *Aquifer characterization techniques: Schlumberger methods in water resources evaluation series no. 4*. Springer Hydrogeology, 671. Switzerland: Springer.
- McCall, G. W., and Christy, T. M., 2010, Development of hydraulic conductivity estimate for the Hydraulic Profiling Tool (HPT): The 2010 North American Environmental Field Conference & Exposition, The Nielsen Environmental Field School, Las Cruces, New Mexico, January 12–15, 2010.
- McCall, G. W., Nielsen, D. M., Farrington, S. P., and Christy, T. M., 2005, Use of direct-push technologies in environmental site characterization and ground-water monitoring; *in* D. M. Nielsen, ed., *The Practical Handbook of Environmental Site Characterization and Ground-Water Monitoring*. 2nd ed.: Boca Raton, Florida, CRC Press, p. 345–472.
- McCall, W., and Christy, T. M., 2020, The Hydraulic Profiling Tool for hydrogeologic investigation of unconsolidated formations: *Groundwater Monitoring and Remediation*, v. 40, p. 89–103, <https://doi.org/10.1111/gwmr.12399>.
- Morozov, D., Walsh, D., McLaughlin, C., Nguyen, A., Grunewald, E., Caldwell, W., Pipp, D., Basore, N., Christy, T., and Macedo, J., 2024, High-resolution direct push NMR tools for groundwater investigations: *Groundwater Monitoring and Remediation*, v. 44, p. 39–54, <https://doi.org/10.1111/gwmr.12645>.